LTR-00-AP-021

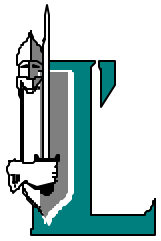

L'Garde, Inc.

Large Telescope Using a Holographically-Corrected Membrane Mirror

Final Report to the NASA Institute for Advanced Concepts (NIAC)
November 2000

Research Grant No. 07600-050
Prime Contract No. NAS5-98051

Prepared by:

Arthur L. Palisoc, Ph.D.
NIAC Fellow/Principal Investigator
L'Garde, Inc.

Approved by:

Arthur L. Palisoc, Ph.D.
Manager, Analytical Engineering
L'Garde, Inc.

Gordon Veal
Vice President, Engineering
L'Garde, Inc.

TABLE OF CONTENTS

TABLE OF CONTENTS, Cont'd.

TABLE OF CONTENTS, Cont'd.

1.0 EXECUTIVE SUMMARY

The objective of the Phase I study was to assess the feasibility of using ultra lightweight holographically corrected membranes as the primary mirror for a large aperture astronomical telescope. The conclusion of the study is that (a) holographically corrected membrane telescopes (HCMT) are eminently feasible and (b) they are the only **affordable** method today and in the foreseeable future enabling diffraction-limited space-based large aperture telescopes. We believe that the concept is revolutionary in the manner defined by the NASA Institute for Advanced Concepts (NIAC). If this concept were to be demonstrated for large apertures in space, and there is no reason why it could not be, it could revolutionize observational astronomy.

In a related NRO (National Reconnaissance Organization) study, a non-inflated 1m diameter parabolic membrane mirror was designed, fabricated, and measured to be within the 1 mm rms surface accuracy limit prescribed. The surface inaccuracy was measured to be $\varepsilon = 0.367$ mm rms which is well within that which could be fully corrected holographically. The NRO study has also proven, at least on a small scale, that the non-inflated net-less membrane mirror design is workable and can attain the required surface accuracy. Scalability to larger diameters was carried out analytically by performing a finite element simulation on 10m and 20m apertures. The analysis included the result of thermal calculations using TRASYS and SINDA. The results of the thermal calculations show that the use of extremely low CTE (coefficient of thermal expansion) PBO membrane combined with a sun-shielded telescope design results in low temperature gradients over the membrane mirror surface and temperatures remaining practically constant in time as long as the relative orientation between the sun and the telescope remains the same.

The 1m NRO membrane mirror was holographically corrected to the diffraction limit. After correction, the focal spot was diffraction limited. Its use as a diffraction-limited imaging device, was demonstrated by illuminating a USAF resolution chart with diffuse laser light and a photograph taken.

The perimeter truss design for the membrane mirror support structure is in Section 4.0. Here, we leveraged off the Large Radar Antenna (LRA) program with NASA/JPL. LRA is a current L'Garde program and is addressing the support structure materials and design for large space structures (~50m). The packaging and deployment control of large apertures will be addressed in detail during Phase II. The perimeter truss (PT) like the membrane mirror is foldable and packageable into a small launch volume. The PT is made of inflatably deployed material that rigidizes by passively cooling the structure to a temperature below its glass transition, Tg. The Tg of the resin used for the PT boom elements has been shown by the LRA program to be *tailorable*, up or down the temperature scale.

A conceptual design of a 1m diameter holographically corrected membrane telescope is presented in Section 9.0. The system issues are addressed and include (a) bandwidth, (b) temporal correction (fixed or real time holography), (c) holographic media, (d) laser beacon distance from the telescope, (e) laser beacon power and pointing requirements, and (f) laser beacon platform (co-orbiting or fixed). A conceptual design of the optics module is also presented. The overall conceptual design of a sun-shielded 1 m HCMT consists of the primary mirror, a holographic correction module, associated optics, and a co-orbiting laser beacon platform. Photopolymer material was chosen as the holographic medium because of its sensitivity to the laser frequency, high resolution, availability, low cost, heritage, and non-wet processing requirement. UV light is used to "fix" the hologram. For ultra high resolution research like planetary imaging, extraterrestrial planet search, deep sky surveys, etc., a more distant orbit such as the L2 Lagrange point would be required for lower thermal and gravitational gradients.

Finally, we outlined and listed some of the many applications of a narrow bandwidth telescope such as an HCMT. Very narrow band imaging and spectroscopy do have applications in astronomy but only for relatively bright sources. By using ultra lightweight membrane mirrors, we could increase the aperture diameter many fold to compensate for faint sources, without much mass penalty and launch vehicle constraint.

The applications address some of the NASA missions under the Space Science Enterprise (SPE) including (a) Search for Origins, (b) Structure and Evolution of the Universe, and (c) Exploration of the Solar System. Some of the applications considered are:

(A) Detection of extra-solar planets. The small angular separation between the planets and their host stars, as well as their extreme differences in brightness makes the detection very difficult. A large HCMT will make it possible to observe medium sized planets in the extra-solar neighborhood.

(B) Cosmology. Larger telescopes will allow us to resolve finer details and view fainter objects which in turn allows us to more accurately define the Hubble constant, the density of the universe, the cosmological constant (if it exists) and hence the age and future of the universe.

(C) Solar system objects. With a 100m diameter space telescope, we could observe every planet in our solar system with more detail than any previous fly by mission. We could also use the large telescope as an early warning device in finding and locating near-earth objects especially those that could intersect the earth's orbit around the sun.

(D) Black hole environs/accretion disks.

(E) Sun spots and solar flare activity on nearby stars.

(F) Red and brown dwarfs.

(G) Galactic, stellar, and planetary formation regions.

(H) Astrometry. Astrometry requires high resolution measurement without the requirement of large bandwidth imaging. The number of stars observed by the Hipparcas/Tycho mission conducted by the European Space Agency (ESA) was ultimately limited by the size of the telescope aperture. For future catalogs, essential in the era of ultra large telescopes, large aperture astrometry missions will be required. HCMTs are well suited to this application.

(I) Optical communications. Experiments have shown that holographically corrected telescopes can be used for optical transmitters/receivers. In fact, as a consequence of the hologram, which is both a narrowband phase plate as well as a dispersive element, HCTs have the potential to isolate signal frequencies much better than conventional telescopes and with fewer optical elements. Signal bandwidths of 100 GHz have been demonstrated with >60dB blocking, with further improvements possible with holographic media.

(J) Lidar. Lidar involves the detection of scattered laser signal from some distant source. Since this source is often gaseous, the return signals are often so low that either a large laser pulse or large receiver (or both) is required. A large receiver can reduce the required laser power required. The results from optical communications tests show that HCTs can be used for lidar receivers, with many improvements over existing systems.

For astronomy, perhaps the most intriguing science would be due to the unexpected. Most discoveries made with new telescopes have been due to seeing the previously unobserved. We know the Hubble Deep Field showed images of galaxies far younger than other telescopes have detected before and with a dramatic increase in both resolution and light gathering power. An ultra large telescope aided by the membrane primary mirror and a holographic correction as outlined in this report will no doubt see a host of new objects and processes in our mysterious universe.

2.0 OVERVIEW OF PHASE I STUDY

2.1 Objective of the Phase I Study. The objective of the Phase I was to carry out an assessment of the feasibility of using an ultra lightweight reflective membrane as the primary mirror of a large aperture astronomical telescope. Although thin film technology is a fast growing technology field, its impact on membrane mirrors may never come to the point where membranes can have the surface accuracy required of an orbiting astronomical telescope. The revolutionary solution we proposed to enable orbiting, space based large aperture telescopes was the use of membranes for the telescope mirror and correcting it to the *diffraction-limit* using a holographic technique. In the related NRO study, we fabricated and demonstrated the full correction of a 1 m diameter, F/D=2.43 membrane mirror. We strongly believe the method to be scalable to 100 meters.

2.2 Introduction. To answer some basic science questions about the origin of the universe and the possibility of life in other parts of the Solar System and beyond, it is necessary to build much larger telescopes than those available today. The *Hubble Space Telescope* (HCT) with its 2.4 m primary mirror has provided significant information about outer space during the last 10 years but much higher resolution is required to unlock the secrets of the universe.

Large aperture, lightweight, space-based telescopes are required for next generation systems to increase the resolution of space targets. A large diameter telescope, on the order of 10m or larger is needed. Of course people have talked about using distributed apertures, which allegedly would get rid of single large aperture problems. Unfortunately, this concept introduces much more significant problems than it solves. The requirements on time and space accuracy imposed on the individual spacecraft making up this distributed architecture will be very difficult to overcome with the foreseeable technology of the future. Thus, we are back to large apertures. However, large apertures manufactured and based on current materials technology for telescopes are heavy, bulky, and very expensive. At this time, *ultra low expansion* (ULE), *silica*, and *zerodur* are the three most commonly used materials for space telescopes and mirrors and only ULE is used for large apertures. Evolutionary improvements in the manufacturing of these materials cannot provide larger blanks to make much larger mirrors. However, the space community, including the intelligence and the military have an insatiable demand for higher and higher resolution images. This demand can only be met by a revolutionary approach. It is necessary to abandon the traditional evolutionary approach and look *outside the box* for other techniques and concepts to develop a large diameter telescope.

Secondly, once the space telescope is manufactured, one is faced with the problem of delivery of the article into orbit. It is not the payload mass that is usually of concern but the packaged volume. For example, space shuttle payloads are almost never weight constrained but volume constrained. The largest booster fairing diameter including the Shuttle cargo bay cannot accommodate an aperture size on the order of 10 m or larger. This makes the launch cost of large aperture systems prohibitively expensive. The telescope must be package-able in a small volume for delivery into orbit after which it is

deployed to its full diameter. This is where membrane mirrors have a clear advantage. Not only are they lightweight, they are also *volume-conformable* as well as package-able in a much smaller volume.

2.3 Proposed Solution. An aberrated mirror has been shown to be correctable to the diffraction-limit using a holographic technique.[1] A mirror fashioned out of a thin film membrane can be made to approximate a parabolic or spherical surface but to be useful as a telescope mirror in the optical regime, the surface inaccuracy and surface slope errors need to be extremely small. By itself, membrane mirrors do not have the required accuracy but coupled with a holographic-correcting technique, it can be made to work in the diffraction-limit. However, there is an upper bound to the surface inaccuracy that the holographic procedure can correct. During the last few years, polymeric materials with extremely low CTE such as polybenzoxazole (PBO) have been predicted to have an on-orbit surface inaccuracy of only 0.35 mm rms. At the same time, holographic techniques have been improved considerably to the point that surface inaccuracies on the order of 1 mm rms or less are perfectly correctable to the diffraction limit.[1,2] It must be noted that membrane reflectors on the order of 10m diameter made from Kapton-E with ten times larger coefficient of thermal expansion (CTE) than PBO, have been shown to have ~1 mm rms surface inaccuracy. And this includes ALL sources of errors on orbit including thermal effects. Hence, a spherical or parabolic mirror made of a thin film of PBO in conjunction with the proper holographic correction can enable a 10m or larger space-based aperture operating in the diffraction limit.

3.0 HOLOGRAPHIC CORRECTION OF ABERRATED MIRRORS

3.1 Holographic Correction. The proposed solution is to construct an astronomical telescope from a lightweight membrane mirror, which is holographically corrected for surface distortions, *in-situ.* This scheme makes it possible to correct apertures of virtually unlimited size, over a narrow bandwidth, at optical and UV wavelengths. This technique has previously been demonstrated for conventional telescopes, microscopes, and communication transceivers. As can be seen in Section 8.0, the method works as well for a membrane mirror.

The basic operation of a holographically corrected reflecting telescope is shown in Fig. 3.1. It has been shown that poor mirrors can be corrected to the diffraction limit using this technique. There are limitations however. These are (1) a collimated beam is used as reference, implying that there already exists a source of (laser) monochromatic light at some distance away to create the reference beam. Such a scheme would involve deploying the laser as an isolated device, or as an instrument fixed to the International Space Station (ISS). (2) Because the hologram is made at a specific laser frequency, the correction is maximized only at that frequency.

Testing and analysis have shown that the first limitation can be softened by using a laser reference beacon located at the center of curvature instead of a collimated beam, but this technique introduces errors into the correction. Similarly, the bandwidth of light that can be handled can be increased, again with some reduction in accuracy.

As shown in Fig. 3.1, a distant source of laser light (the beacon) is used to illuminate an aberrated primary with the focused light directed through a secondary optic that collimates the light and produces a de-magnified image of the primary onto the holographic medium (Fig. 3.1a). A hologram is recorded between this object beam and a diffraction-limited plane wave reference beam incident at an angle. If light from a distant object is incident on the primary (Fig. 3.1b), a reconstructed beam will be produced which can be focused to form an un-aberrated image of the distant object. This technique is used to remove aberrations present in a large diameter, inexpensive optical system to produce a diffraction-limited telescope operating over a moderate bandwidth. Furthermore, the same scheme can be used for any type of primary – reflecting or refracting, parabolic, spherical, or any other conic.

A hologram is a record of the distortions of the primary at any given time, and can correct for these distortions, as long as no changes occur to the mirror between recording and replay. In a space environment, thermal and gravitational gradients will produce minute changes in the shape of the membrane mirror, which means that a single static hologram cannot permanently correct for an aberrated primary. There are several solutions to this problem, including real-time holographic media such as *optically-addressed spatial light modulators* (OASLM) or *photopolymer* materials, or incorporating an inexpensive adaptive optics system in conjunction with a high resolution static holographic medium.

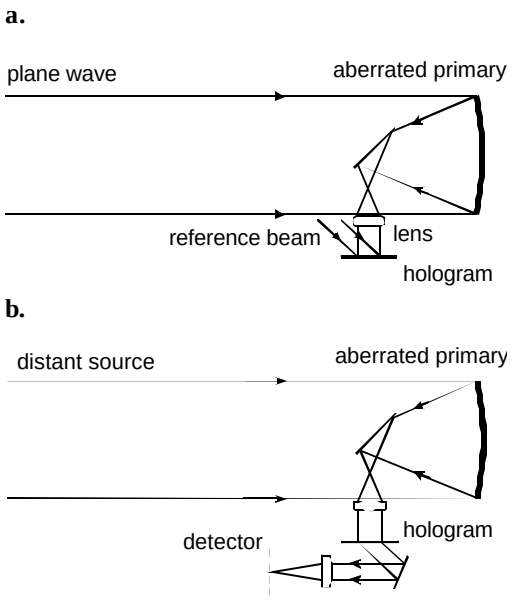

Fig. 3.1. A schematic of a holographically corrected telescope. a.) Recording. A distant laser source illuminates the aberrated primary to form the object beam. The hologram is written with a collimated beam incident at an angle. b.) Reconstruction. Light from a distant object (starlight) reconstructs an unaberrated image which is then focused to produce a perfect image of the distant object.

Photopolymer materials are perhaps the most desirable media, as they are very inexpensive, very lightweight, and can be used for either real-time or static holographic correction in a space environment. To create a hologram using a photopolymer film, the film is exposed to the laser light and developed using UV. A hologram (from a light-proof *roll* of photopolymer film) is simultaneously recorded and reconstructed to adapt for temporal changes in the shape of the primary. New holograms from the same roll can be created as needed.

3.2 Previous Holographic Results. Holographically corrected telescopes have been extensively investigated [4-8] with many different designs and apertures as large as 0.5m. Figure 3.2 shows the result of correcting a 0.5 m diameter telescope mirror. This is reproduced from Ref. 9. The reproduced copy shown is not as high quality as the original. The telescope was tested as an imaging instrument by placing a resolution chart at the focus of the parabolic collimator and illuminating it with diffused laser light. Diffraction limited resolution was obtained after correction.

These demonstrations show that mirrors with as much as 1 mm rms departure from a perfect figure can indeed be completely corrected using holograms, which is critical in systems involving lightweight, membrane primaries. The same holographically corrected telescope has been shown to be ideal for optical communications, with possible data transfer rates beyond 100 Giga bits per second (Gbps).

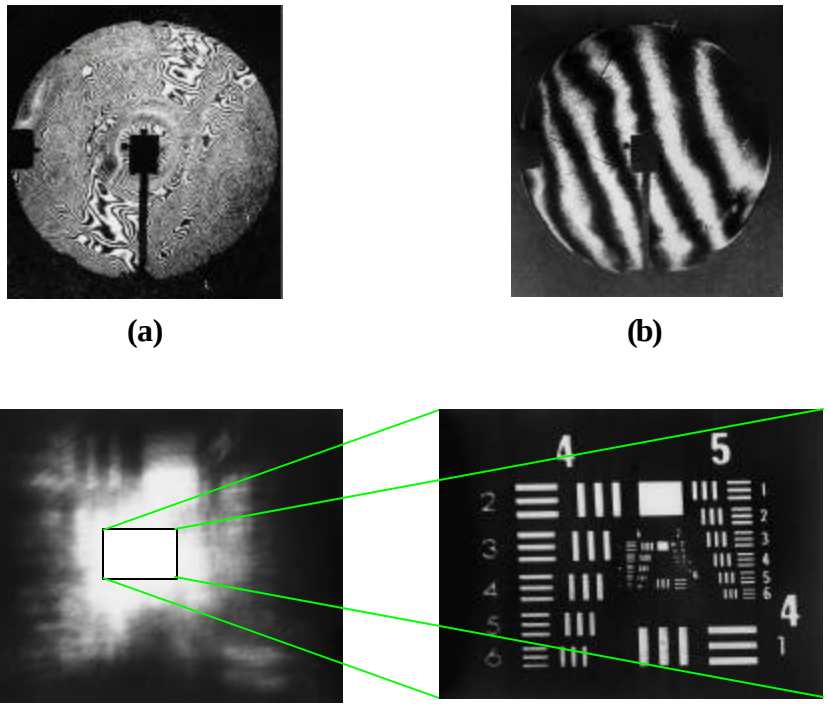

Fig. 3.2. **:** Holographic correction of a 0.5m diameter mirror. The interferometric pattern **a.** before, and **b.** after showing the removal of 250 waves of aberration. A 1951 USAF resolution test chart **c.** before, and **d.** after correction.

Recently, Andersen, et al. [2] demonstrated the complete removal of over 2500 waves of aberration in a 0.2 m diameter, F/2.5 spherical primary mirror, to diffraction-limited performance. Figure 3.3 below shows the results of the experiment.

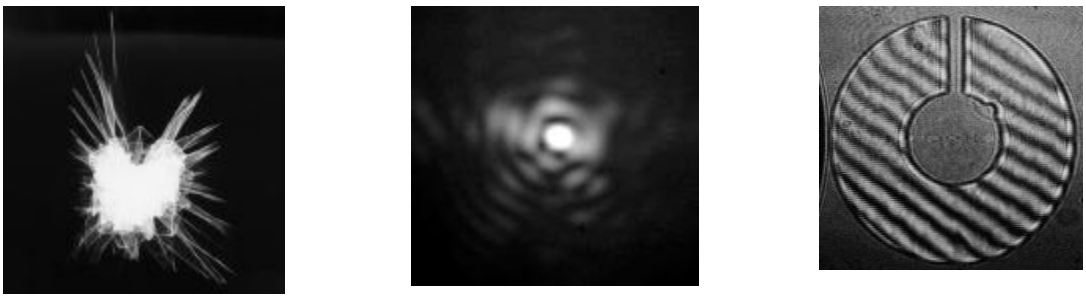

Fig. 3.3. Imaging. (a) The uncorrected focal spot, shown actual size. (b) The focal spot of the reconstructed beam, shown magnified by 500X. (c) Wavefront. An interferogram of the reconstructed beam, indicating better than diffraction limited performance. Due to the overwhelmingly large error to begin with, no "before" interferogram was possible for comparison.

4.0 ADVANCED CONCEPT DESCRIPTION

4.1. Net-Membrane and Net-Less Membrane Mirror. A 10m aperture, lightweight, space-based telescope is required to revolutionize space exploration and unlock some of the mysteries of the universe. The ultimate objective is to manufacture a payload consisting of a 10 m or larger telescope in a compact configuration that can be integrated with a platform to produce an operational flying imaging spacecraft to revolutionize space exploration. In Fig. 4.1 we show three different membrane mirror configurations. The first (Figs. 4.1 A and B) is the purely inflatable reflector. It is a lenticular structure consisting of a reflector membrane and a clear canopy. The lenticular volume is pressurized with inflatant gas that strains the reflector membrane smoothing out the packaging wrinkles. The second and third concepts are non-inflated: the *net-membrane* and the *net-less* configurations. The *net-membrane* configuration consists of the reflector surface, which is formed by a net-membrane structure. The net forms a geodesic surface over which the metallized reflector membrane is stretched. Another net structure but without the membrane, is located at the "bottom" and is a mirror image of the top net. This bottom net is used as anchor points for tension ties between it and the top net-membrane. These ties provide tension in the membrane keeping it taut and wrinkle-free. The net material is an accurately built low CTE, high stiffness composite network and provides the accuracy and added thermal stability. The perimeter truss support structure can be made of a light, deployable, rigid composite material or inflatable rigidizable material. The *net-less* configuration like the net-membrane, is non-inflatable. It is similar to the net-membrane but as its name suggests, it does not have a cable matrix (net) over the reflector surface. The reflector surface is tensioned via tension ties bonded to the back of the reflector and the other end anchored to a net structure at the "bottom". Because there is no cable network over the reflector, there is some weight savings as well as increased light gathering area.

4.2. Perimeter Truss Support. The membrane mirror support structure is the perimeter truss shown in Fig. 4.2. Here, we leveraged off the *Large Radar Antenna* (LRA) Program with NASA/JPL that is currently addressing the perimeter truss configurations for large space structures. Most of the design and analysis of the perimeter truss supports have been done within the LRA program.

The perimeter truss type that is suitable for a 10 m diameter or larger aperture is the *Diamond* truss shown in Fig. 4.2A. In Fig. 4.2B, we show the *net-membrane*. Since the conical truss concept –Fig. 4.2C – offers the possibility of further reducing the mass and packaging volume, we have included it as a good perimeter truss candidate.

The perimeter truss support structure shown in Figs. 4.1C and D are made of inflatably-deployable, rigidizable material. One such candidate uses the *Sub-Tg* method of rigidization. That is, prior to deployment, the material is at a temperature above its glass-transition temperature (Tg) and hence it is flexible and foldable. After deployment, it is allowed to (passively) cool below its Tg making the material very stiff and rigid. L'Garde has identified a radiation-resistant resin for use in impregnating graphite fabric for making Sub-Tg trusses.

(**A**)

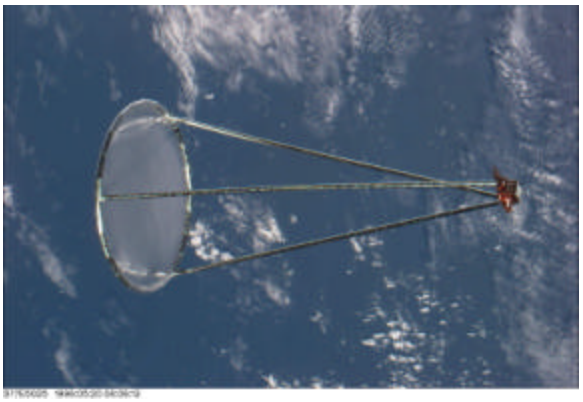

(**B**)

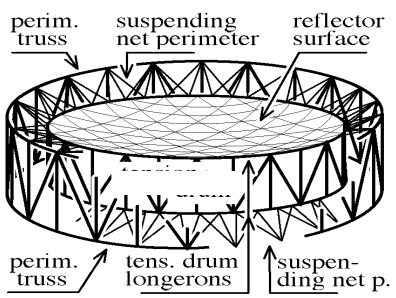

(**C**)

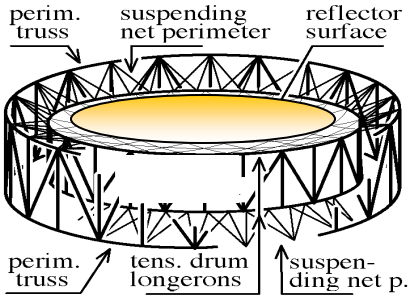

(**D**)

Fig. 4.1. (A) and (B). Purely inflatable membrane mirrors. The inflatable reflector shown in (A) is 7 m in diameter with an F/D=0.5. It is a ground model. The inflatable reflector shown in (B) is the Inflatable Antenna Experiment (IAE) on-orbit. It was deployed by the Space Shuttle STS-77 on May 20, 1996. It is the first ever inflatable reflector flown in space. (C) Net-Membrane mirror shown with its perimeter support structure. The struts are not shown. (D) Net-less membrane mirror shown with its perimeter support structure. The struts are not shown.

In the Phase I study, we carried out the design and analysis of the *net-membrane* configuration. The *net-less membrane* configuration was addressed by the related NRO study. The results of the finite element analysis of the *net-membrane* and *net-less*

configurations are presented in Section 7.0. In the NRO study, a 1m diameter net-less membrane mirror was fabricated and its surface profile was measured using videogrammetry. The fabricated membrane mirror was successfully holographically-corrected to the diffraction limit. The results of the holographic tests can be found in Section 8.0.

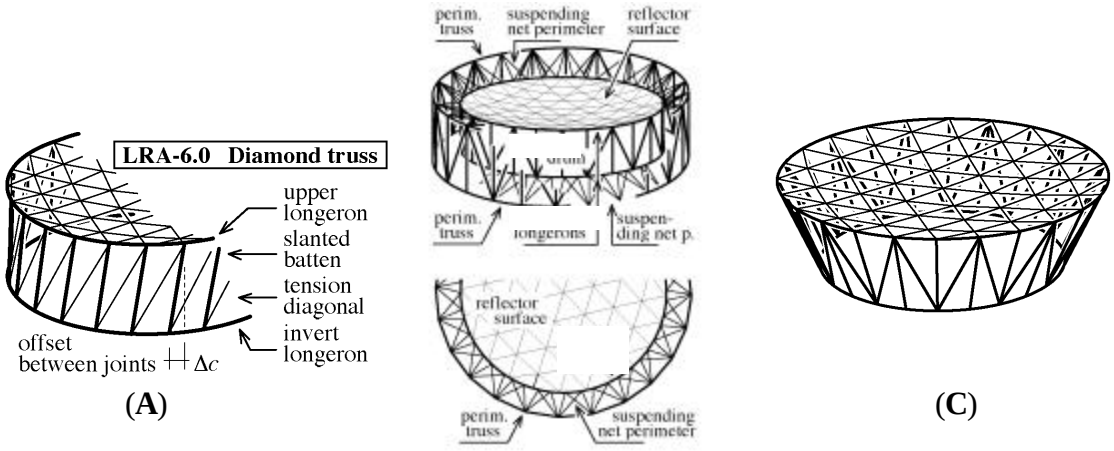

Fig. 4.2. Perimeter truss support for the membrane mirror telescope. (A) Diamond truss. (B) Net-membrane mirror supported by a perimeter truss. (C) The conical perimeter truss.

5.0 TECHNOLOGY CHALLENGE

5.1. Surface Accuracy. There are issues and challenges to the technology regarding the use of membrane mirror for optics.[3] The first and foremost is surface accuracy. The current state of the art on-orbit precision for membrane reflectors up to about 10m aperture diameter using Kapton-like material is on the order of 1 mm rms with ALL sources of surface degradation considered including manufacturing and thermal effects. At smaller diameters (≤3m), 0.5 mm rms accuracies have been achieved on ground measurements. Figure 5.1 shows some of the (inflatable) membrane reflectors that L'Garde, Inc. has built to date. The last one, Fig. 5.1D, was built under the NRO program and is the non-inflated *Net-Less Membrane Mirror*.

5.2 Membrane Material. For a space application, the membrane material for the mirror must be able to resist the hazards of the space environment; e.g. atomic oxygen (at low earth orbits), radiation, UV, and micrometeoroids. On top of this, the thermal excursions experienced by the membrane mirror must be such that its surface profile changes are still correctable holographically. Moreover, the transient component of the temperature effects must be "slow" enough to render the hologram constructed for that particular state usable over the entire time interval of astronomical/astrometry observation. Therefore, a very low coefficient of thermal expansion (CTE) membrane material is needed. Fortunately one such material exists. It is polybenzoxazole (PBO). For such low CTE materials ($\alpha \approx -1$ ppm/C°), an on-orbit surface accuracy of 0.35 mm rms has been predicted for aperture diameters of 10m. These error magnitudes have been shown to be holographically-correctable to the diffraction limit.[1,2] PBO however, unlike Kapton E, has not yet been tested for space radiation resistance. Kapton-E was shown to be resistant to space radiation (GEO levels) for a mission life greater than 5 years.[14] Analytical calculations, though, predict that PBO should be slightly more radiation resistant than Kapton-E.[15] What remains now for PBO film membrane is to be tested for space environment resistance.

5.3. Holographic Film Material. In order to accomplish holographic correction in real-time and *in-situ*, we need a suitable holographic film material. The holographic film material must also be able to resist the harsh environment of space that include radiation, UV, micrometeoroids, and at low earth orbits, atomic oxygen. In designing a holographically corrected membrane telescope (HCOMET), the holographic film material can be shielded against atomic oxygen and most micrometeoroids. However, it may not be possible to completely shield it against radiation. Hence, whatever holographic film material is chosen, these issues must be seriously considered. Section 9.0 discusses the different holographic media and issues associated with each of them

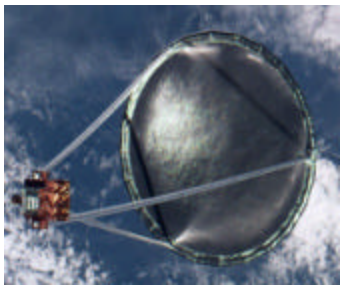

(**A**)

(**B**)

(**C**)

Fig. 5.1. (A). The Inflatable Antenna Experiment (IAE) Reflector on-orbit. Deployed from the Space-Shuttle on May 20th, 1996, it is the first ever parabolic membrane reflector to be flown in space. (B). One-fifth sector of the IAE reflector – 3m diameter. This membrane mirror was ground tested and measured to have a surface accuracy of 0.67 mm rms. It was used to test the IAE Surface Accuracy Measurement System (SAMS). (C) Three meter diameter HAIR (Highly Accurate Inflatable Reflector) reflector. This was fabricated in the late '80s and had a measured surface accuracy close to 1 mm rms. (D) One meter diameter *Net-Less* membrane mirror. This mirror was fabricated for the NRO and was measured videogrammetrically to have a surface accuracy of 0.367 mm rms. It was also holographically corrected to the diffraction-limit.

(**D**)

5.4 Perimeter Support Structure Material. The perimeter support structure material is baselined on a Sub-Tg resin impregnated graphite fabric. When the material is at a temperature above its glass-transition temperature (Tg), the composite laminate is soft, flexible, and packageable. Hence, a small amount of power may be needed from the parent spacecraft to keep the payload at the required temperature. After deployment, it is exposed to the space environment and allowed to (passively) cool below its Tg making it very stiff and rigid. A modulus of a few million psi has been obtained using the Sub-Tg method. A radiation-resistant Sub-Tg resin with the proper glass transition temperature is required. L'Garde's research into this has so far resulted in the identification of one candidate resin. Although its Tg is high, about 30 °C above room temperature, the good thing is that its Tg is tailorable. Work is continuing to synthesize a (radiation-resistant) resin with a low Tg. The LRA program at L'Garde is currently addressing this issue.

6.0 THERMAL ANALYSIS OF THE 1 M DIAMETER MEMBRANE TELESCOPE

6.1 Thermal Model. It is imperative that we know the temperature profile over the membrane mirror. Any distortion of the mirror primary will impact the imaging capability of the optical system. Furthermore, we must know the magnitude of the distortion to determine whether or not they are within the capability of the holographic correction method used. The thermal analysis presented here is by no means complete. The time and budget for the Phase I study did not permit a more thorough analysis. As such, the simple analysis carried out in this section is aimed to give us an indication of the temperature and temperature gradient magnitudes to expect on-orbit.

The thermal model is shown in Fig. 6.1. The 1 m diameter membrane mirror is shown encased in a tubular sunshield. One end of the sunshield is open to allow light from a distant target, a star, planet, etc. to get into the holographically-corrected membrane telescope. The membrane mirror is made out of 0.005 inch (12.7 micron) thick PBO membrane.

6.2 TRASYS Model. An orbit altitude of 220 nautical miles was assumed for the 1m diameter membrane mirror. TRASYS [16] was used to estimate the thermal loading on the telescope. The input to TRASYS consists of the geometry of the model, the optical properties, the orbit (earth-centered or sun-centered), the altitude, and the orientation of the spacecraft (the model) relative to the heat sources. TRASYS also allows the user to extract the radiation conductors within the model itself as well as the radiation conductors to space; i.e., the conductor(s) with one end connected to a node at the temperature of outer space. In this case, we used absolute zero. These conductors as well as the irradiation of each of the elements are then used in as subsequent SINDA[17] run to calculate the temperature-time history of the elements of the thermal model. The parameters of the thermal model are listed in Table 6.1. The model has been simplified in that the perimeter truss structure had not been included. This is not expected to change the temperature results of the membrane mirror.

6.3 SINDA Model. SINDA [17] is a finite difference thermal analyzer and is widely used in the aerospace industry. Input to the code consists of the thermal network and the nodes specifications. The network is defined by specifying the conductor (or thermal resistor) values between interconnected nodes. For the nodes, the capacitance and initial temperature (if a transient analysis) must be specified as well as the type of node; i.e., diffusion, arithmetic, or boundary. In the SINDA run, the initial temperature of the boom nodes have been specified to be 70 °F = 21.1 °C.

Our main interest is the temperature and temperature distribution within the membrane mirror material. In particular, we want to know if the operating temperature is within the tolerance of the material itself. Secondly, are the temperature gradients within that which can cause distortions beyond what is holographically correctable? Within the membrane telescope thermal model, we used 45 nodes - 9 nodes per quadrant and 36

circumferential (linear) conductors and 24 axial (linear) conductors. The telescope cylindrical enclosure is covered with MLI and the effective emissivity between the MLI and the telescope tubular enclosures is taken as $\varepsilon^* = 0.02$.

Table 6.1. Parameters of the Thermal Model.

Geometric Properties	
Membrane mirror diameter	1 m
Sunshield diameter	2 m
Overall Length	3.05 m
Telescope F/D	2.43
Mass and Physical Properties	
Sunshield material density	1.8 g/cm^3
Sunshield specific heat	921 J/kg-C
Membrane mirror material density	1.38 g/cm^3
Membrane mirror specific heat	921 J/kg-C
Membrane mirror thermal conductivity	0.173W/cm-C
Optical Properties	
Outer sunshield surface	
Emissivity	0.269
solar absorptivity	0.58
solar transmissivity	0
Inner sunshield surface	
emissivity	0.90
solar absorptivity	0.90
solar transmissivity	0
Membrane mirror surface	
emissivity	0.05
solar absorptivity	0.15
solar transmissivity	0
Effective emmisivity used for MLI	0.02
Number of conductors within the Cylindrical tube	14,758
Number of conductors within membrane Mirror	60
Number of conductors to space	468

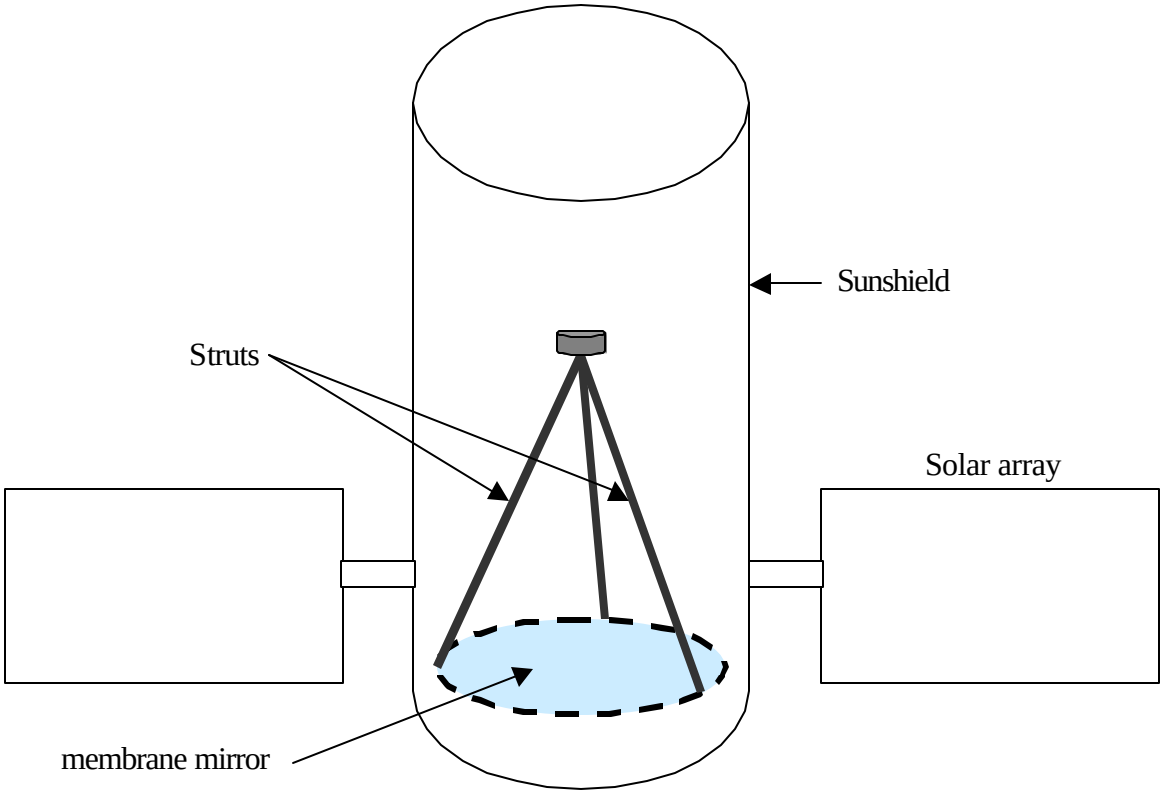

Fig. 6.1. The thermal model of the 1 m diameter holographically-corrected membrane telescope on-orbit.

6.4. Results. Because the membrane mirror is so thin, its thermal mass is very small. We then expect its temperature to get to its operating temperature almost as soon as it is exposed to the thermal environment. This is indeed the case as shown in Fig. 6.2B. The orbit was assumed to be a 220 nautical mile altitude circular orbit with the sun directly overhead. The irradiation of the model was calculated by TRASYS. This was subsequently input to SINDA for the calculation of the temperatures.

As can be seen from Fig. 6.2B, the temperature of the membrane mirror drops almost instantaneously – as soon as it is exposed to its thermal environment. The temperature remains constant throughout. This is expected because the irradiation is constant. The sun is always overhead and the telescope is always pointing away from the earth. It will also be noted that the largest temperature gradient over the membrane mirror is less than 9 C°. This gradient can be reduced with better insulation around the telescope. The temperature over the membrane mirror shown in Fig. 6.2B were obtained with an effective emissivity of $\varepsilon^* = 0.02$ between the MLI and the telescope tube. With the CTE of the membrane material being $\alpha = -1 \times 10^{-6}$ /C° the change in the mirror surface will still be within what can be holographically corrected. The surface accuracy after the application of the thermal loads changed negligibly, from $\varepsilon = 0.401$ to 0.399.

However, the focal length increased slightly, as expected. Since the membrane shrunk due to the drop in temperature, the mirror focal length increased.

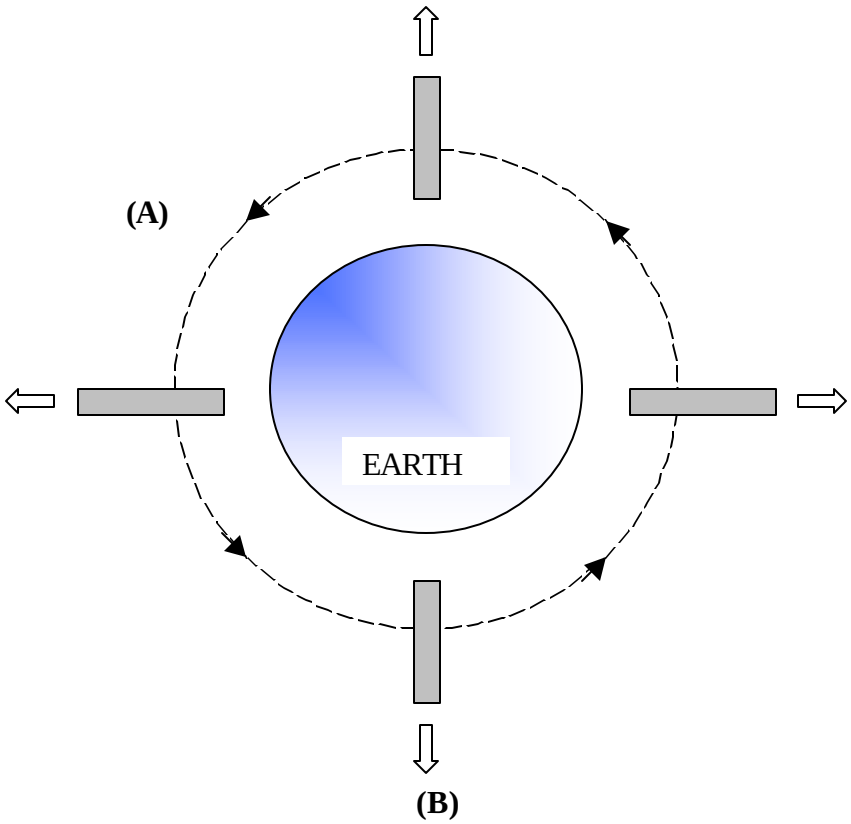

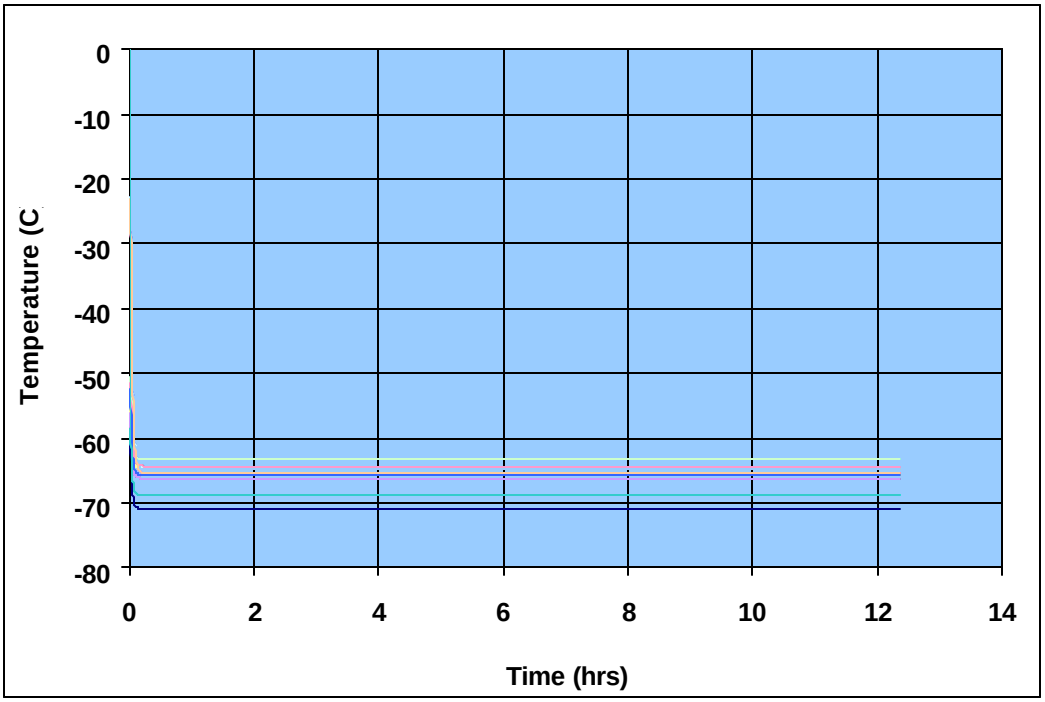

Fig. 6.2. (A) 220 nautical mile circular orbit. Sun is assumed directly overhead. (B) Temperature –time history of selected nodes on the membrane mirror. Note how quickly the temperature drops and stabilizes.

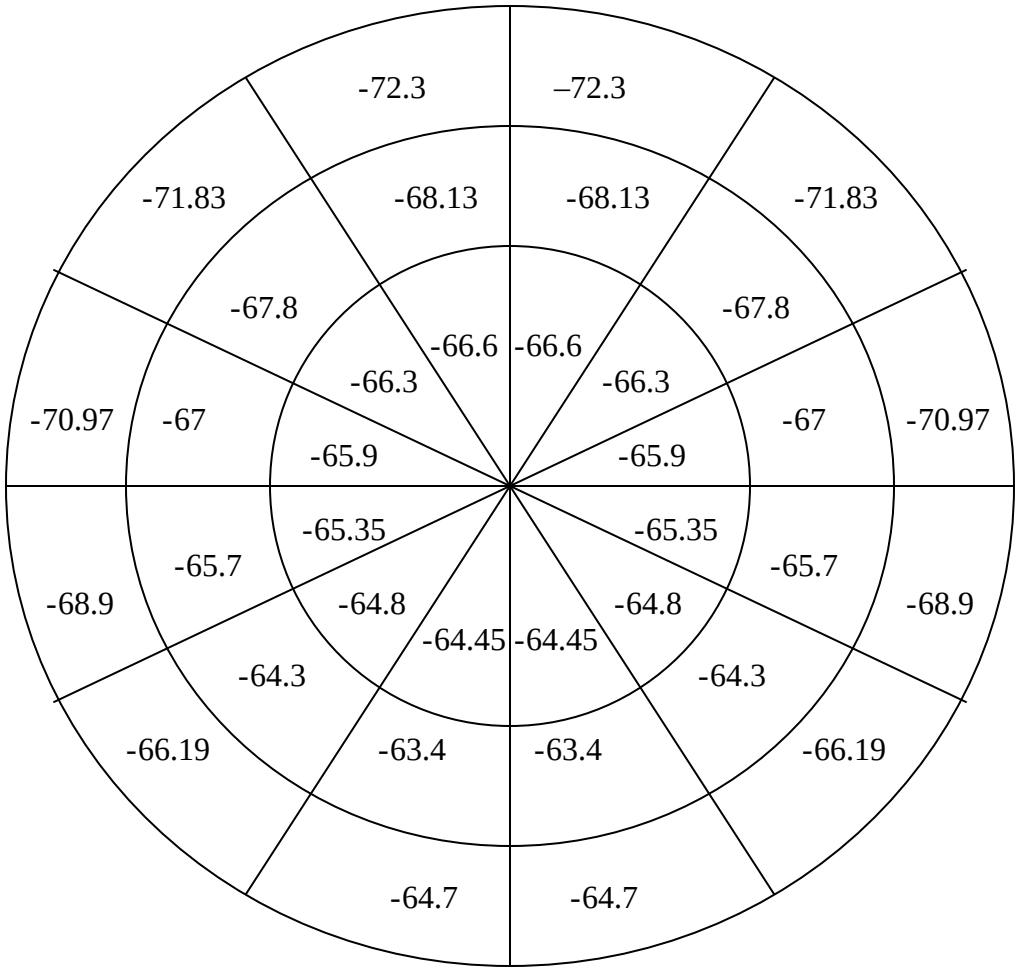

Fig. 6.3. Temperature distribution over the membrane mirror. The numbers in each SINDA cell are the temperature of the cell in degrees Celsius.

7.0 FINITE ELEMENT MODELING OF THE MEMBRANE MIRROR

7.1. Finite Element Analysis. In order to assess the structural performance and predict the surface accuracy of membrane mirrors in a space environment, we carried out a finite element analysis (FEA) of the *Net-Membrane* and the *Net-Less* configurations. We used the FEA to predict the surface profile of the 1m diameter Net-Less membrane mirror built for the NRO study. We extended the calculations to assess the scalability of the concept by analyzing a 10m and a 20 m diameter aperture, *Net-Membrane* configurations. For the *Net-Less* configuration, we carried out the analysis for a 1m and a 10 m size aperture.

7.2 Finite Element Model of the *Net-Membrane* Mirror. Fig. 7.1A shows the finite element model of a 10m diameter *Net-Membrane* mirror. The surface contours are shown in Fig. 7.1B. The model contains 1731 nodes, 832 membrane elements, and 634 cable elements. This model used 853 tension ties. The overall predicted surface accuracy is ε = 0.142 mm rms. A finite element model was also created for the 20 m diameter. Because of symmetry (60° symmetry) only a 60° slice of the circular parabolic membrane is modeled.

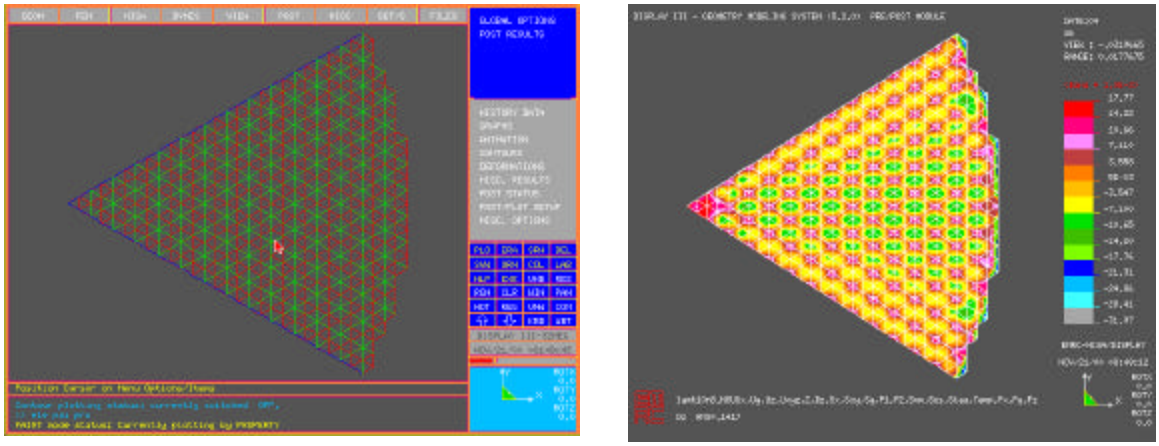

(A) **(B)**

Fig. 7.1 A. Finite element model of 10m Net-Membrane mirror. B. Predicted surface profile of 10m Net-Membrane.

7.3 Finite Element Model of the *Net-Less Membrane* Mirror. Fig. 7.2A shows the finite element model of the 10m *Net-Less* membrane mirror. The surface contours are shown in Fig. 7.2B. The model contains 3459 nodes and 1092 membrane elements. The overall predicted surface accuracy is 0.39 mm rms. This model used 1215 tension ties. Note that the predicted surface accuracy for the Net-Membrane (Fig. 7.1) is better than for the Net-Membrane. We can increase the surface accuracy of the Net-Less by

increasing the number of tension ties. However, from the fabrication point of view, this may not be practical.

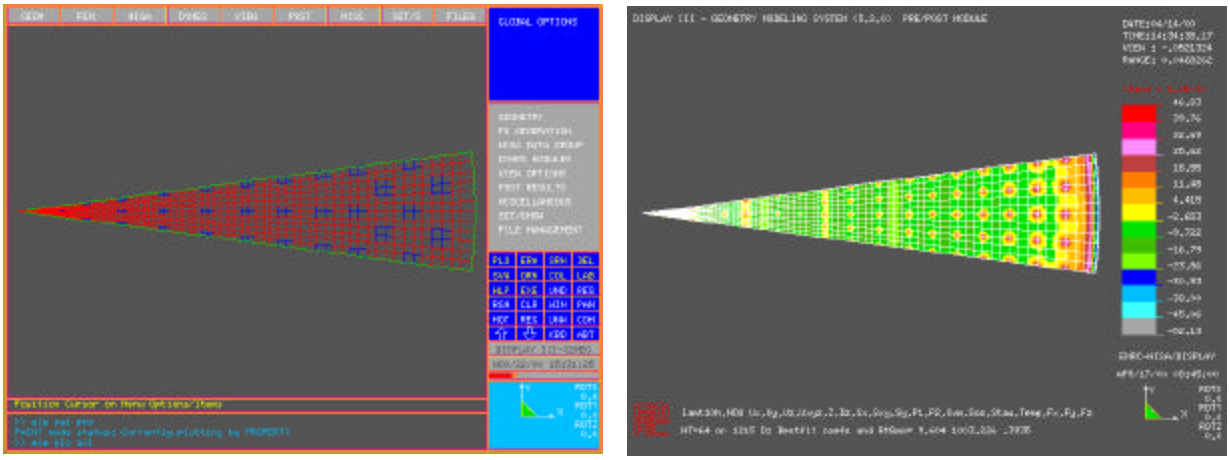

(A) **(B)**

Fig. 7.2. A. Finite element model of 10m Net-Less membrane mirror. B. Predicted surface profile of 10m Net-Less membrane mirror.

A 1m diameter *Net-Less* Membrane mirror was fabricated for the NRO study. The mirror is shown in its fabrication steps in Fig. 7.3. The *Net-Less* configuration is similar to the *Net-Membrane*, except that the *Net-Less*, as the name implies, does not have a cable network over the reflector surface. In order to strain the membrane mirror, tension ties are bonded on its backside via plastic tabs. The other ends of the ties are hooked up to the "bottom" of the perimeter truss and the tension adjusted via screw knobs. The backside of the un-tensioned Net-Less membrane mirror is shown in Fig. 7.3A. The tension ties are bonded to the "Kapton side" of the membrane mirror. The tensioned reflector is shown in Fig. 7.3C. This photo angle was used to show more clearly the curvature of the surface. The tiny "dots" on the surface are the retroreflective targets used in the videogrammetric measurement of the surface quality. The material used for the mirror was aluminized (vapor deposited aluminum) Kapton-E. Only one side was aluminized. Fig. 7.3B and 7.3C show the aluminized side.

A thermal load case using the results of Section 6.0 Thermal Analysis, for the 1m diameter case was used in a finite element run. The "before" and "after" cases are shown in Fig. 7.4 – surface profiles. The design temperature used for this finite element run was –60 °C. The "hottest" temperature was about –63 C and the coldest, -72.3 C. Therefore, there is an overall temperature drop relative to the design temperature. This means that the membrane, assumed to be PBO in this case, shrunk. Hence, we should expect the focal length to increase after the application of the thermal loads. This is indeed the case. The surface accuracy and the focal length before and after the load are shown in Table 7.1.

(A)

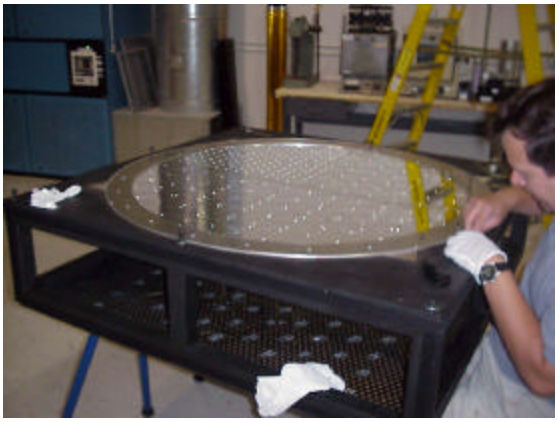

(B)

(C)

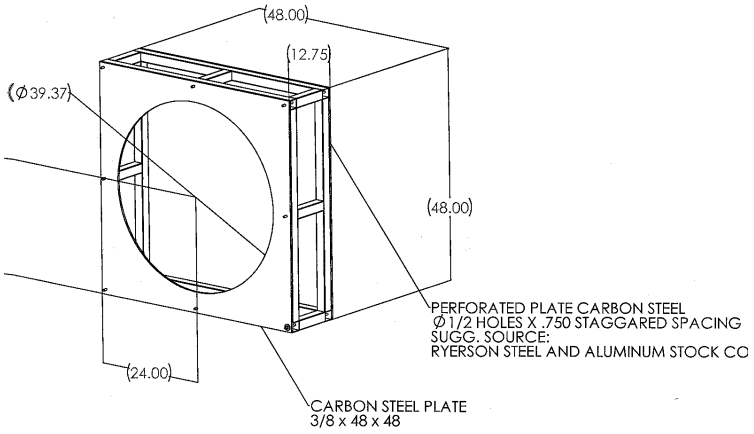

(D)

Fig. 7.3. The 1 m diameter Net-Less Membrane Mirror in fabrication. A. The backside of the mirror is shown with the tension ties bonded but still in its slack state. The mirror at this point is still unstressed. B. The aluminized side of the mirror is shown with the retro targets being (carefully) applied. In C, the tensioned *Net-Less* membrane mirror is shown upright ready to be measured videogrammetrically. This photo angle was chosen to show the double surface curvature achieved. Eight seven ties were used. The measured surface accuracy was $\varepsilon = 0.367$ mm rms with a best-fit focal length of 2.43 m. The F/D = 2.43. D. The support structure used for the 1m *Net-Less* Prototype.

Table 7.1. FEM Simulation of One Meter Diameter Net-Less Membrane Mirror before and after the Application of the Temperature Loads shown in Fig. 6.3.

	Before	After
Focal Length	2.575 m	2.579 m
Surface Accuracy	0.401 mm rms	0.399 mm rms

As can be seen, since the temperature gradient over the membrane mirror surface is very small and the design temperature chosen to be close to the average operating temperature, the overall effect on the mirror profile is small. The magnitude of the effect is still within the range, which can be corrected holographically. The good thing is that for a sun shielded telescope like the model shown in Section 6.0, the temperature gradient over the mirror surface is very small and the temperature stays almost constant over time. The implication of this is that we may need to construct not as many holograms to take into account the otherwise many different *temporal* and *structural* "states" of the mirror. In fact, a sunshield must be used to thermally protect the mirror and achieve the surface accuracies required for holographic correction. The results of the sensitivity analyses are shown in Table 7.2.

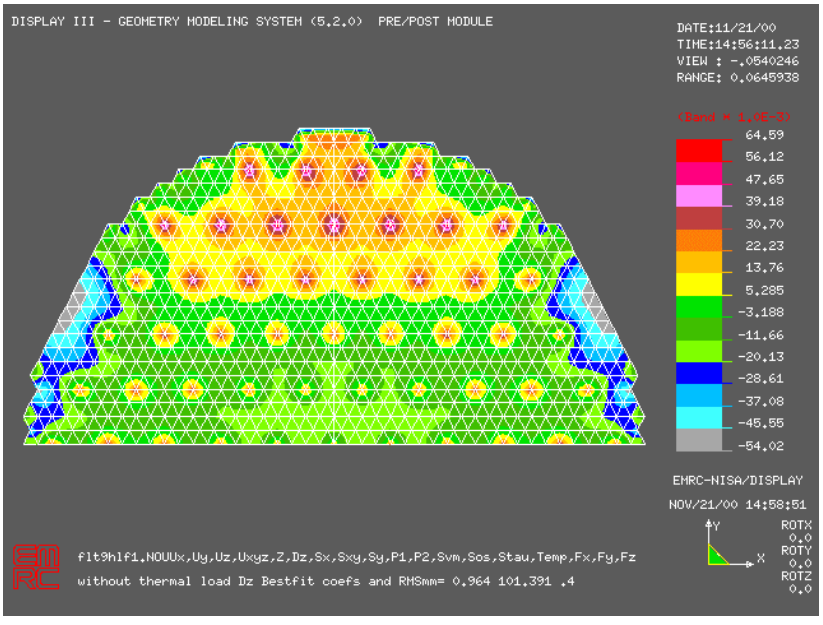

Fig. 7.4 (A)

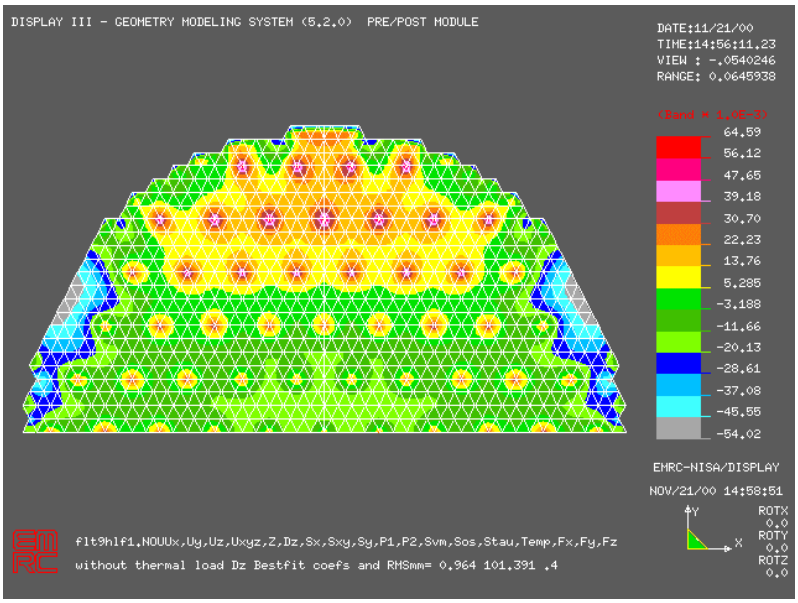

(B)

Fig. 7.4. Thermal Load Case for the 1m Net-Less Membrane Mirror. (A) Before thermal load is applied: F=2.575 m, rms=0.401mm rms. (B) After thermal load is applied: F=2.579m, rms=0.399 mm rms. Because the temperature gradient over the surface is small and the design temperature chosen to be close to the average operating temperature, very little change in the mirror surface profile occurs. The magnitudes of the profile change is still within the limits that can be corrected holographically.

Table 7.2. Results of Sensitivity Analysis for the 10m and 20m Net-Membrane.

	10 m		20m	
No. of Ties	583		847	
	F/D	ε (mm rms)	F/D	ε (mm rms)
Baseline	2.60	0.142	2.60	0.216
A. Random tie force (10%)	2.61	0.183	2.60	0.283
B. Random force directions(5°)	2.60	0.142	2.60	0.216
C. Random net length error†	2.61	0.209	2.61	0.257
Combination of A,B,C	2.61	0.210	2.60	0.318

†Standard deviation = 0.002 inch error for every 25 inch length.

8.0 RESULTS OF HOLOGRAPHIC CORRECTION

In a related study for the National Reconnaissance Organization (NRO), L'Garde built a 1 meter diameter Net-Less parabolic membrane mirror. It is shown in Fig. 7.3C. The objective of the NRO study was to show holographic correction of a membrane mirror to the diffraction limit. In order to achieve the illumination of the entire 1 m diameter aperture with a diffraction-limited beam, a 1 m diameter rigid parabolic mirror blank was polished to 1 wave rms. Its F/D is 2.4. The grinding and polishing work has only recently been completed and at the time of this writing, it is on its way to the Naval Observatory in Flagstaff, Arizona to be aluminized. After the (rigid) mirror collimator is coated, it will be shipped to the USAF Academy Laser and Optics Research Center (LORC), in Colorado Springs. It is at the LORC where the final holographic correction of the membrane mirror will take place. This will happen sometime in mid-December 2000. Because of this, we will not have the full results of the holographic correction of the Net-Less Membrane mirror. The LORC however, has another collimator but with a much lower reflectivity. Whereas we expect about 95% reflectivity on the NRO collimator, the LORC's collimator has a reflectivity of only about 4%. It could still be used but it takes more time and very careful effort to produce the hologram. In fact, this LORC mirror was used and the result of the holographic correction reported here was carried out using the LORC collimator. An addenda section was added to this report where we will add the final holographic test results (using the more reflective NRO collimator) when they come in sometime in January of 2001.

8.1. One Meter Diameter *Net-Less* Membrane Mirror. The *Net-Less* membrane mirror is shown in Fig. 8.1. It is shown under construction in Fig. 8.1A and under videogrammetric test in Fig. 8.1B. Figure 8.1C shows the mirror at the USAFA LORC in Colorado Springs under holographic test using the LORC collimator. The parameters of the Net-Less membrane mirror are listed in Table 8.1.

Table 8.1. Parameters of the 1 m Membrane Mirror.

	Design	Measured
Diameter	1.00 m	1.00 m
F/D	$2.0 < F/D < 2.6$	$F = 95.67 \Rightarrow F/D = 2.43$
Surface Accuracy	$\varepsilon \leq 1.00$ mm rms	$\varepsilon = 0.367$ mm rms

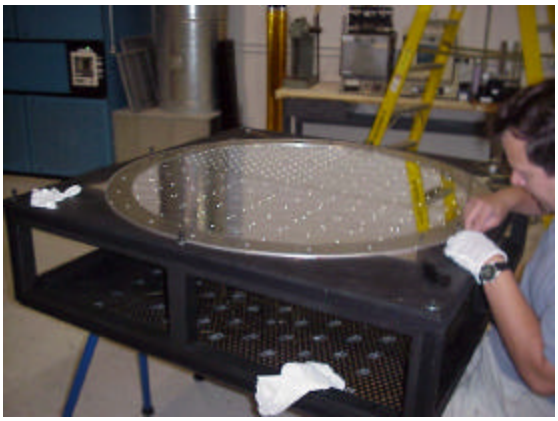

(A)

(B)

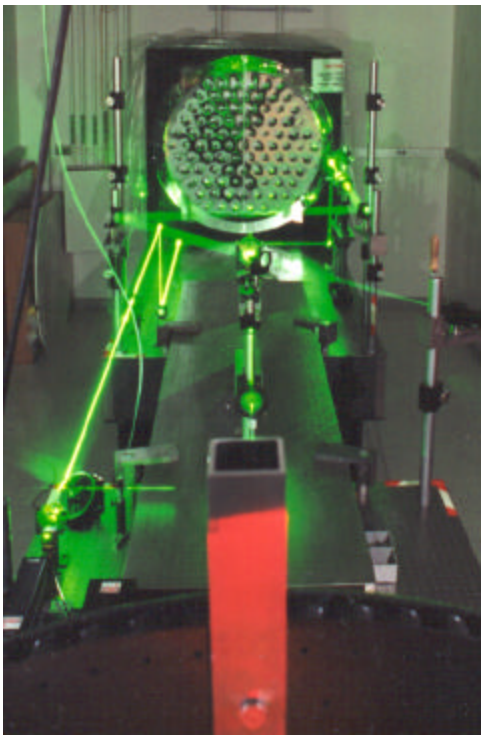

(C)

Fig. 8.1. (A) The Net-Less membrane mirror under construction at L'Garde. (B) Under videogrammetric measurement at L'Garde. Note the double curvature of the surface. The "dots" on the surface are retro-reflective targets used for the videogrammetric measurement. (C) Under holographic correction at the USAFA LORC Laboratory in Colorado Springs.

8.2. Holographic Correction of the Net-Less Membrane Mirror. The holographic correction was carried out at the USAFA Laser and Optics Research Center. The result using the LORC collimator (4% reflective) are shown in Fig. 8.2. The uncorrected focal spot is shown in Fig. 8.2A. It is about 12.5 cm in diameter. Although the mirror has a surface inaccuracy of only 0.367 mm rms, there is a substantial amount of light scattering away from the focal point because the surface slope error is relatively high. A *net-membrane* configuration will probably obtain a relatively more focused spot but it is not clear until a full ray-tracing simulation is conducted. A similar but purely inflatable membrane mirror will achieve an even smaller focal spot.

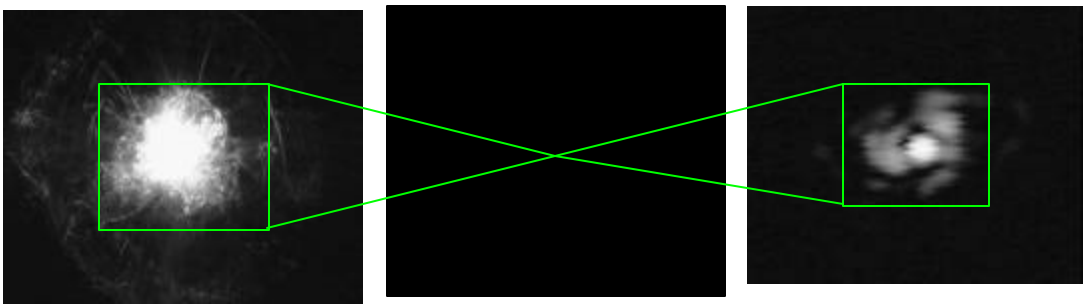

(A) **(B)** **(C)**

Fig. 8.2. Focal spot of 1 m Net-Less Parabolic Membrane Mirror. (A). Before correction, the focal spot size was about 12.5 cm. (B) After correction, a diffraction-limited focal spot was obtained. (C) Focal spot magnified to 750 microns.

A USAF resolution chart was imaged with diffuse laser light and imaged using the holographically corrected membrane telescope mirror. The results are shown in Fig. 8.3. Note that before correction, the image was blurred and unidentifiable. After correction, diffraction-limited resolution was obtained.

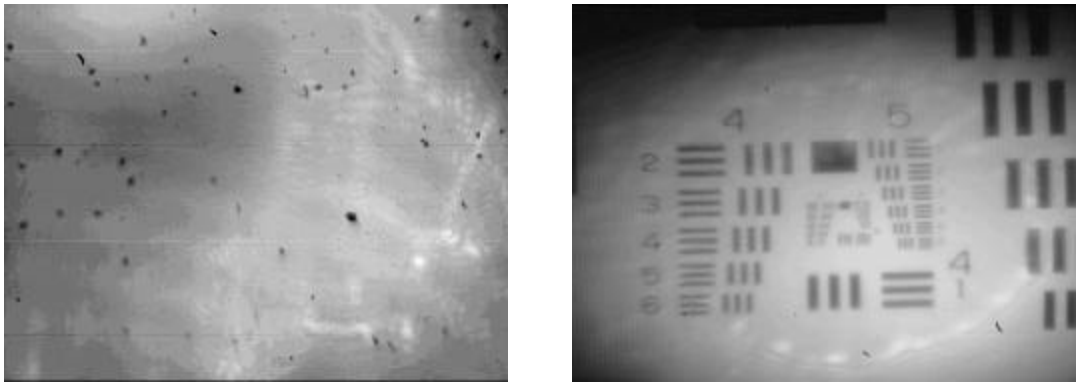

(A) **(B)**

Fig. 8.3. USAFA resolution chart imaged before and after holographic correction. (A) Before. (B) After correction, diffraction-limited performance was obtained.

The results of the correction using the more reflective NRO collimator will be added later in the Addendum Section, Chapter 14.

Below is a simulation using a 100 m diameter holographically-corrected membrane telescope. The figure on the left is an image of Europa, one of Jupiter's moons, taken with the Hubble Space Telescope (HST). On the right is the image of Europa if it were taken with a 100 m diameter holographically-corrected membrane telescope from the same distance.

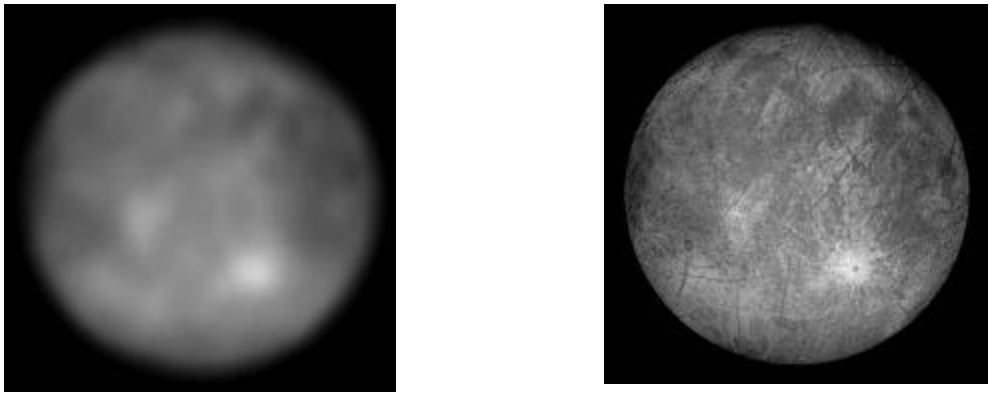

(A) **(B)**

Fig. 8.4. Europa, one of Jupiter's moons. (A) Taken by the Hubble Space Telescope (HST). (B) An image simulation of Europa had it been taken by a 100m holographically-corrected membrane telescope. Notice the much higher resolution.

9.0 CONCEPTUAL DESIGN OF A SPACE-BASED 1 M DIAMETER MEMBRANE TELESCOPE

9.1 Design issues. The basic design for a space telescope will look something like that shown in Figure 9.1. In this section the more specific design issues associated with a space-based HCT will be discussed in more detail.

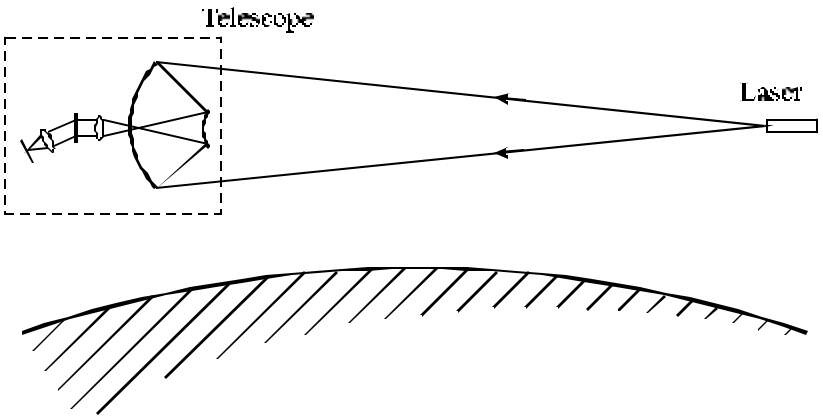

Fig. 9.1. A holographically corrected space telescope. The distant laser beacon illuminates the aberrated telescope from a separate orbiting platform, resulting in the most compact and lightweight telescope possible.

9.1.1 Bandwidth. The hologram is a recording of the phase error of a surface defect at the wavelength of the laser. On reconstruction, this same phase correction, applied to the aberrated wavefront at the same wavelength, will result in complete removal of the aberration. At a different wavelength, however, the same phase translates into a different absolute correction, which will be either more or less than that required. For a recording wavelength, λ_1, the bandwidth, $\Delta\lambda$, is given by:

$$\Delta l = l_1 \frac{Final\_error}{Initial\_error} \tag{1}$$

Thus, with an initial wavefront error of 10 waves, to be corrected to 0.1 waves, the bandwidth will be 1% that of the recording wavelength (i.e. ~10nm at λ_1=1μm). It should be stressed, however, that although complete correction is only possible within this bandwidth, there is still a dramatic reduction in the wavefront error at other wavelengths. Furthermore, this can actually be exploited in some applications such as optical communications, where narrowband operation is desired.

Although the bandwidth at a given wavelength is small, a different hologram can be recorded at several different wavelengths. While this will still provide only a small fraction of the overall spectrum, comparison between images at discrete wavelengths can

still provide large amounts of information about distant objects. In order to record these separate holograms, the beacon laser must be capable of multi-spectral emission. The details of the laser design will be discussed in a later section.

9.1.2 Temporal correction. The hologram will completely correct for the mirror distortions so long as there are no changes in the relative positions of any of the optical components and no changes in the figure error of the primary throughout the lifetime of the hologram. For long-term correction, either the movement must be eliminated, or a method of adjusting for these temporal changes must be devised.

9.1.2.1 Fixed holography. For a rigid mirror, a fixed, one-off holographic medium may be used. In this case, a new hologram may only be required every 1000 hrs or less. Minor thermal or gravitational gradients may only amount to changes of a few waves or more, so in this case, a hybrid system may be preferable, such as the one shown in Figure 9.2 below.

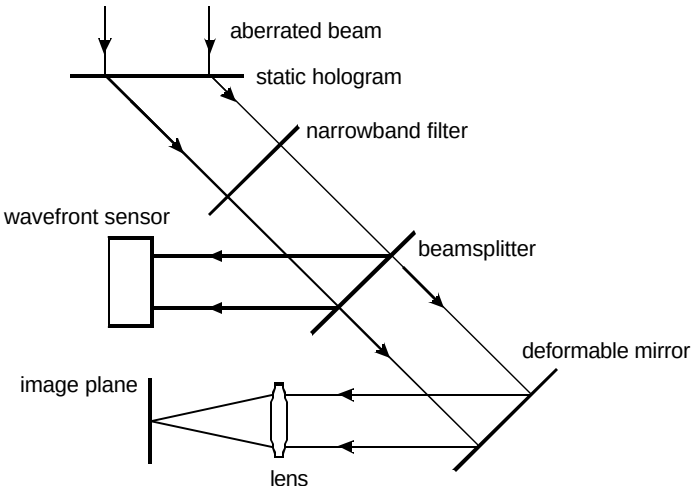

Fig. 9.2. Hybrid holographic correction. The large-scale aberrations are removed by a static hologram, while minor temporal changes in the mirror are corrected by the small-stroke deformable mirror.

The hybrid system uses the large-stroke correction of fixed holograms, with the rapid temporal correction (up to 1kHz) of the small-stroke deformable mirror [18,19]. In the space telescope we are proposing here, the design would initially consist of the fixed hologram only. The modular design concept, however, would allow for replacement of the fixed reflector with the optics necessary for adaptive optics correction.

9.1.2.2 Real-time holography. Any real time holographic correction requires the hologram to be recorded at the same time as it is reconstructed. As such, there is the obvious problem of designing a system with constant beacon illumination, given that the

laser is to be positioned many kilometers away. While there is the possibility of having a beacon located close to the primary, this has been shown to be an impractical solution for primaries with small F-numbers [7,21]. In any case, the fact that there will be laser illumination in the direct line-of-sight of the primary will inevitably reduce the sensitivity of the telescope. Meanwhile, there are also the problems of designing a laser for near-continuous operation, and the need for several individual lasers for multi-spectral correction. As such, for a real time correction scheme, the hybrid system is seen as a more efficient and more robust approach.

9.3 Holographic media. The choice of holographic media depends on the type of correction desired. There are several options, each with advantages and tradeoffs. Table 9.1 shows a comparison of various types of materials.

	SHG[a]	DCG[b]	HRF-600[c]	EOP[d]	SLM[e]
Exposure[1]	0.1	300-1000	0.1	5	4×10^{-4}
Resolution[2]	6000	6000	1000	1000	200
Response time[3]	n/a	n/a	n/a	500	1
Efficiency[4]	90%	100%	>90%	>90%	30%
Grating type[5]	V, T	V, T	V, T	V, T	V, R
Processing[6]	Wet	Wet	Dry	Dry	n/a
Overwrite[7]	N	N	N	Y	Y
Substrate[8]	G, C	G	G, P	G	G
Lifetime[9]	>1000	>1000	>1000	>1000	>1000
Stability[10]	Good	V. good		V. good	V. good
Outgassing[11]	Y	Y			N
Max. size[12]	100	>500	>200	50	35
Scatter[13]	Low	V. low	V. low	Low	V. low
Wavelength[14]	400-650	300-500	400-520, 630-660		400-850

Table 9.1. Properties of optically addressed holographic media (blank cells indicate unknown quantity, n/a indicates not applicable).

1. Typical exposure in mJ/cm^{-2}
2. Resolution in line pairs per mm
3. Response time (msecs) for realtime performance
4. Maximum efficiency (ratio of 1st diffracted order to input)
5. T: Thin, V: Volume, T: Transmission, R: Reflection, S: Relief (surface)
6. Wet: Chemical processing, Dry: Non-chemical processing
7. The media's ability to be reused for more than one hologram
8. G: Glass, C: Cellulose, P: Plastic/Polymer
9. Hologram lifetime with minimal change in performance (in hours)
10. Stability of hologram performance over thermal range of 10-30°C

11. Possibility of outgassing from medium or substrate
12. Maximum size (in mm) of hologram possible with currently available samples
13. Qualitative measure of amount of scattered light
14. Typical operating wavelength in nm

a. Silver halide sensitized dichromated gelatin
b. Dichromated gelatin
c. DuPont Omnidex holographic recording materials[22,23]
d. Electro-optic photopolymers[24]
e. Optically addressed spatial light modulators[9,25]

For a space telescope, wet processing is impractical, which leaves photopolymers as the most likely candidates (assuming a fixed/hybrid system is adopted). The DuPont photopolymers have fairly good performance characteristics and are a well-tested technology, and as such would be the most logical short-term choice for a holographic medium. The photopolymer will be held in *light-proof rolls*, so that it can be wound out for exposure any time new film is required.

9.4 Beacon

9.4.1. Distance. The recording scheme requires a distant source of coherent light (the beacon). Exactly how distant this laser beacon needs to be depends on the dimensions of the primary to be corrected. With the beacon located some finite distance away, there will be some spherical aberration present on recording (for a parabolic primary, for example). If, on replay, a source at infinity is to be viewed, there will be no spherical aberration present. Since the hologram has some spherical aberration recorded, it will be present on the reconstructed beam, giving less than perfect performance. The magnitude of spherical aberration (to 3rd order) for a mirror with a semi-diameter ρ, focal length f, and a beacon distance y, is given by:

$$W = \frac{(y - f)\rho^4}{8 f^2 y^2} \tag{2}$$

Figure 9.3 shows how the wavefront error changes with beacon distance for 1m diameter mirrors of various different F-numbers.

Given the large beacon distances involved, it may seem that a HCT is quite infeasible. However, in a space environment, where atmospheric distortion is not an issue, the beacon distance is largely irrelevant and only affects the pointing stability requirements for the laser. Since it possible to calculate the amount of uncorrected spherical aberration, it is also possible to incorporate the removal of some of the error in secondary optics, in much the same way as was achieved with the Hubble Space Telescope, COSTAR system. In this way, we can take a beacon distance of around 50 km and an F/2.0 primary mirror.

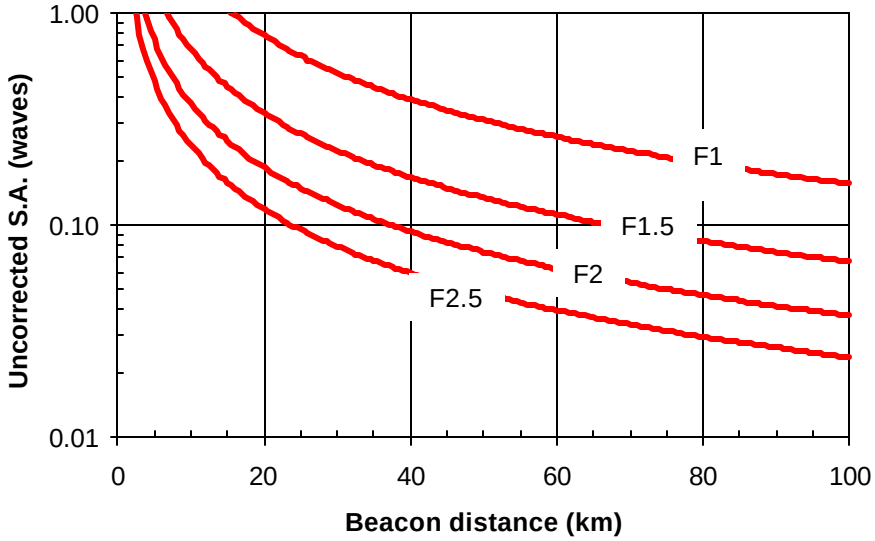

Figure 9.3. This plot shows the amount of uncorrected spherical aberration that remains for a given beacon distance. The mirror diameter is 1m, and the curves show F-numbers of 1,1.5,2 & 2.5 from top to bottom.

9.4.2. Laser platform. The laser platform is expected to be an independently controlled platform, co-orbiting with the telescope. There is the possibility of mounting the laser to the International Space Station (ISS), which would simplify many design issues, but for this analysis we will assume this is not possible.

The laser would have a series of capacitor banks that could be charged by small amounts of current over the long periods of idle time between operation. Other power requirements for the module (such as low-gain communications) are expected to be minor. As such, the power should be fully provided by solar panels on the exterior of the module itself, or by using solar panels if necessary.

A high quality star tracker and gyros will be required for good pointing stability. It may also be necessary to have a simple optical detector attached to the front of the module as a safety backup, to ensure that the laser is never activated while pointed at the Earth. Assuming a diffraction limited laser beam with an initial aperture size of 20mm, we can calculate the beam diameter at 50 km to be 1.7 m, which would require a pointing accuracy of 12 mrad, or 2.5 arcsec. For comparison, the fine-guidance sensors on HST can give an absolute pointing accuracy of 14 arcsec. Unlike those sensors, however, a long-term lock need not be established, since the exposure time is only 10ns. A high

degree of pointing accuracy can also be achieved by pulsing the laser at very low powers, and maximizing the signal received at the telescope.

9.4.3. The Laser. The laser will most likely be a Q-switched system with a pulse length of around 10ns. This will permit a *relative* motion between the laser and the telescope platforms of $10ms^{-1}$. So long as the orbital "altitude" of the two platforms differs by less than 16.7km (~10 miles), the relative velocity between them will be less than this value (assuming a 600km orbit).

The precise laser power depends entirely on the size and medium chosen for the hologram. If we assume a 100mm-diameter hologram, with a required exposure of $0.1mJ/cm^2$, the laser power required will have to be around 350mJ. This value, which takes into account the previously mentioned divergence expected from a 20mm beam at a distance of 50km, is an easily obtainable power with current lasers.

The sole restriction on the beacon wavelength is that a hologram can actually be recorded. Thus, the laser wavelength is determined mostly by the sensitivity of the medium chosen. It is expected that multi-line operation will be desired, so there will need to be some method for converting the natural laser emission wavelength into other wavelengths. This can be achieved by Raman shifting in a multi-stage laser. A Q-switched, frequency-doubled Nd:YAG laser (532nm green) with two external stages which can be added: 1. A Raman shifter for 633nm red. 2. A tripler (to get 355nm) and Raman shifter for 416nm blue. One possible arrangement of this type is shown below in Figure 9.4.

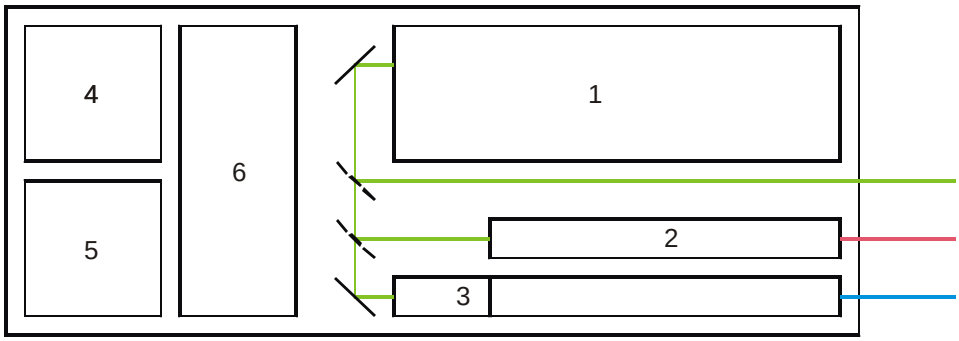

Figure 9.4. The laser module. 1 Pulsed, frequency-doubled Nd:YAG laser, 2 Raman cell, 3 Tripler and Raman cell combination, 4 Star tracker/gyros, 5 Communications/processor, 6 Capacitors. The dotted lines indicate mirrors which can be electronically moved in and out of position. Not shown are the solar cells on the outside of the module.

9.5. Primary mirror. The primary mirror and support struts are designed to be packed within a small volume at one end of the optics module, as shown in Figure 9.5.

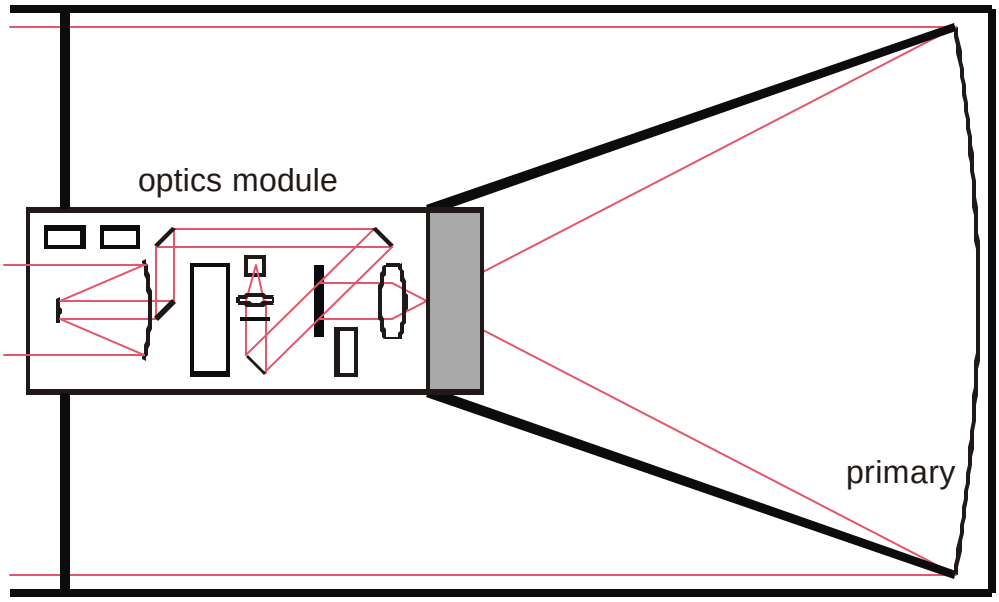

Fig. 9.5. The telescope. The telescope consists of an optics module and the primary mirror enclosed within a protective outer casing. The primary mirror will deploy from the shaded section at the end of the optics module.

The design of the membrane mirror has been discussed in previous sections, but some mention should be made of the choice for the mirror conic. With a distant beacon, any conic can be used for the primary. For example, if a spherical figure is adopted, the spherical aberration, which is present, is treated simply as another aberration to be corrected by the hologram. So long as the spatial frequency of this error does not exceed the maximum resolution of the hologram, complete correction is assured. This allows us to relax the design constraints on the primary figure design somewhat, though obviously the closer the figure is to a paraboloid, the smaller the total wavefront error recorded, and the greater the final bandwidth. The choice of mirror F-number will depend on many factors such as a trade-off between surface figure and minimizing the overall length of the telescope for greater stiffness.

9.6. Optics module. A basic outline of the components in the optics module is shown in Figure 9.6. The telescope used to collect light for the reference beam must be a high quality instrument of about 10-inch diameter. The UV lamp is required to "fix" the hologram in the photopolymer, and is on a translation stage so that it can be placed directly in front of the film. The film itself is stored in a canister and wound down into position when a new hologram needs to be recorded. There will need to be a method of

applying a slight tension to the film in order to ensure that it is rigid and flat. The filter is required to remove light at other wavelengths than those within the correction bandwidth of the hologram. A filter wheel can be used for multi-wavelength operation.

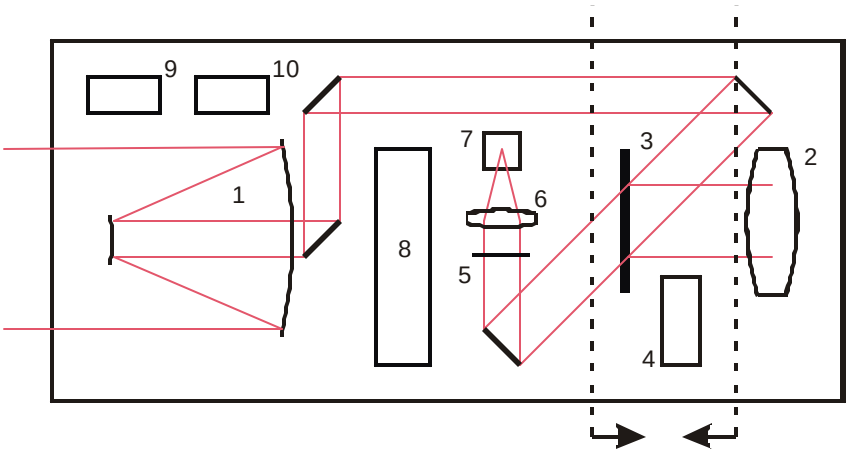

1. 10" Cassegrain telescope
2. Secondary lens
3. Hologram
4. UV lamp
5. Filter
6. Imaging lens
7. CCD
8. Processor/power control
9. Star tracker/gyros
10. Communications

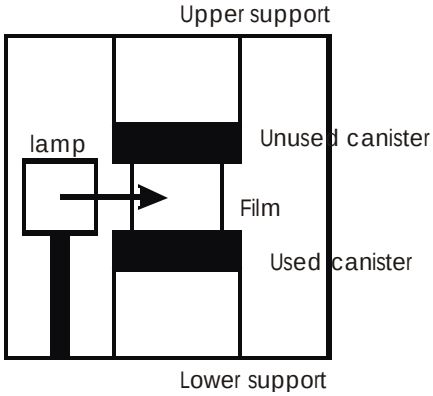

Fig. 9.6: The optics module. The red line indicate light paths through the optical components. The overall dimensions will be ~0.4mx0.4mx1m. A sectional view of the hologram and UV lamp are shown as well.

9.7. Orbit/Servicing. For the lightest possible structure, the telescope can be an open-truss which removes the need for a massive enclosure – see Section 4.0. As in any space telescope, the holographically corrected membrane mirror would still require protection from direct solar radiation for optimum performance. If an open-truss were used, the fixed solar shield would mean the telescope would have to be placed in a polar orbit. If a low-inclination orbit were preferred, an enclosed telescope would be needed.

The design of both the laser and telescope platforms may be modular, enabling future missions to service any parts that fail over the lifetime of the instrument. It is envisioned that this modular design would be much like that for the Hubble Space Telescope. To place an instrument in a polar orbit is a very expensive proposition, so with the

requirements of servicing, the low-inclination orbit (with an enclosed telescope) is set. For a larger diameter telescope such as a 10m or 20m, an altitude above most of the earth's atmosphere is required because of the drag issue. Again, if servicing is required, the higher altitudes are an expensive proposition.

9.8. Future missions. Future holographically corrected telescopes will no doubt incorporate a primary aperture of >10m diameter in order to truly exploit the benefits of this technology. Even a 10m optical telescope would have twice the resolution as the NGST [26] (for less than 10% of the mass) since it would be designed to operate at short optical wavelengths. For ultra-high resolution research (planetary imaging, deep sky surveys etc.), several changes will have to be made for optimum performance. For example, a more distant orbit (such as the L2 Lagrangian point) would be required for lower thermal and gravitational gradients. This would make it possible to return to an open-truss, and low-mass sun-shield design, while removing the possibility of servicing missions.

10.0 ASTRONOMY AND ASTROMETRY APPLICATIONS FOR HOLOGRAPHICALLY-CORRECTED MEMBRANE MIRROR TELESCOPE

10.0 Mission applications. The bandwidth limitations of holographically corrected telescopes make them unsuited as multi-spectral instruments. However, the gains in resolution possible with ultra-large apertures have dramatic benefits for other applications. In many of these, the reduction in bandwidth can actually be used to improve performance over conventional instruments.

10.1 Astronomy. While the narrow bandwidth will not allow for spectroscopic observations, the following is a discussion of the many advances in astronomical science that could be achieved from an ultra-large space-based HCT.

We are at present (and for Phase II) investigating different methods of increasing the bandwidth such as (a) the use of secondary adaptive optics system, (b) the use of pre-formed membrane mirror gores, and (c) several smaller more precise membrane mirrors separated by large distances to increase resolution.

10.1.1 Extra-solar planets. With the indirect detection of over 50 extra-solar planets, there is a great interest in both the scientific and public communities to obtain direct observational data. The small angular separation between the planets and their host stars, as well as their extreme differences in brightness makes this very difficult. In fact, calculations show that even the Next Generation Space Telescope will be unable to image even the brightest of these planets. A much larger HCT will make it possible to observe medium sized planets in the extra-solar neighborhood.

10.1.2 Cosmology. Larger telescopes are able to resolve finer details and view fainter objects which in turn allows us to more accurately define the Hubble constant, the density of the universe, the cosmological constant (if it exists) and hence the age and future of the universe. For instance, the Hubble constant can be measured by observing standard candles such Cepheid variables and/or Type I supernovae in distant galaxies of known redshift. While the redshift of the parent galaxy can be obtained from ground-based spectroscopic instruments, the luminosity of the individual stars and supernovae cannot be detected because of resolution limits. A HCT with an aperture >10m could extend the observational limit for these standard candles and greatly improve the accuracy of cosmological models.

10.1.3 Solar-system objects. Perhaps one of the greatest applications of the Hubble Space telescope will be in observing objects within our own Solar system. With a 100m diameter, space telescope, we could observe every planet in better detail than any previous fly-by mission.

10.1.4 Other observations. With purely high-resolution observations, we can be sure that an ultra-large space telescope would be able to observe many phenomena in more detail, such as:

a. Black hole environs/accretion disks
b. Sun spots on nearby stars
c. Red and brown dwarfs
d. Galactic, stellar and planetary formation regions

Perhaps the most intriguing science would be due to the unexpected. Most discoveries made with new telescopes have been due to seeing the previous unobserved. We know the Hubble Deep Field showed images of galaxies in the universe far younger that other telescopes, and with a dramatic increase in both resolution and light-gathering power, an ultra-large telescope will no doubt see many other new objects.

10.2 Astrometry. Astrometry requires high-resolution measurements of star positions but without the requirement of large bandwidth imaging. The largest catalogue of this type is the Hipparcos/Tycho mission conducted by the European Space Agency, which concluded in 1996. The number of stars observed was ultimately limited by the size of the telescope aperture. For future catalogues, essential in the era of ultra-large telescopes (both ground and space-based), larger aperture astrometry missions will be required. Holographically corrected telescopes will be well suited to this application.

10.3 Optical communications. One of the most promising applications for holographically corrected telescopes is for high-bandwidth optical communications. Increasingly there is a need for free-space networks using optical frequencies for improved data transfer. Areas in which such communications could be useful are not limited just to civilian and military communications. Scientific payloads on spacecraft are capable of collecting much more data than can be transmitted using radio frequencies (e.g. live video feeds). Given the possibility of constructing a lightweight, inexpensive optical communications system, there is the potential for orders of magnitude more data collection from future space missions.

Experiments have shown that holographically corrected telescopes can be used for optical transmitters/receivers. In fact, as a consequence of the hologram, which is both a narrow-band phase-plate as well as a dispersive element, HCTs have the potential to isolate signal frequencies much better than conventional telescopes and with fewer optical elements. Signal bandwidths of 100GHz have been demonstrated with >60dB blocking, with further improvements possible with alternative holographic media.

10.4 Lidar. Lidar is a remote sensing technique increasingly being developed for space-based operations. Applications of lidar include atmospheric profiling (including temperature, wind velocity and aerosol density), species identification and surface profiling. Lidar data is used for turbulence avoidance systems, meteorology and precision mapping/topology. Since most lidar applications support or even require narrow bandwidth detection, holographically corrected telescopes are ideal for such systems.

Lidar involves the detection of a scattered laser signal from some distant source. Since this source is often gaseous, the return signals are often so low that either a large laser pulse or a large receiver (or both) is required. In many aerospace-based applications, where the laser is pointed towards the ground, ocular damage due to direct laser exposure is a serious concern. A larger receiver can reduce the required laser power required. The results from the optical communications tests show that HCTs can be used for lidar receivers, with many improvements over existing systems.

11.0 PHASE II TASKS

Our proposed solution to addressing some of the NASA missions especially the Space Science Enterprise is to carry out a system design of a space-based 100m diameter holographically corrected membrane mirror telescope. We will address the system issues, the enabling technologies, estimate the cost of such a system, and create a technology roadmap whose predicted maturation points will be used as milestones along the timeline culminating in the development, fabrication, and flight of a 100m HCMT. A description of the tasks to accomplish the objectives are enumerated below.

Task 1. Conceptual system design of a 100m diameter HCMT. We have accomplished some elements of this task during this Phase, but for a much smaller HCMT – a 1m diameter. The system design will be performed with a specific NASA mission in mind, e.g. an alternate to the *Terrestrial Planet Finder* (TPF) Mission under the *Search for Origins* of the *Space Science Enterprise*. For other applicable missions, we can identify the changes that need to be made to the baseline design. It is also under this task where we quantify the requirements on the different system components. For example, the capability of the secondary adaptive optics (Task 2) will dictate the requirements on the stiffness of the overall structure which in turn sets the requirement on the stiffness of the other sub-components. Feeding into this task also are Tasks 3, thermal analysis, and Task 4, Finite element simulation of the 100m HCMT.

Task 2. Holographic correction with secondary adaptive optics. Under this task, we will investigate the use of adaptive optics in conjunction with holographic correction. One concern with any use of membrane primaries is that they are susceptible to changes in figure due to thermal, vibrational and gravitational gradients. This problem is not altered by the application of holographic correction. The hologram is a record of the primary mirror aberrations *at the time of exposure*: so long as the system geometry stays constant, there will be complete correction. If the primary mirror changes shape in any way, the hologram will continue to subtract the recorded wavefront aberration, with the net difference in the two wavefronts being present on the reconstructed beam. There are two methods of overcoming this problem: real-time holography and adaptive optics.

There has been much development of real-time holography based on optically addressed spatial light modulators (OASLMs). Using these devices, the hologram can be simultaneously recorded and reconstructed, adjusting for temporal changes in mirror deformation. These devices, however, can only correct for relatively small figure errors (few tens of waves) and have maximum throughput efficiencies of ~35%. The major drawback, however, may be the requirement of having continuous laser illumination. In this way, the laser beacon must always be in front of the object being viewed.

A more practical approach is to use conventional static holography with high efficiencies (~100%) and high spatial definition, allowing several thousands of waves of surface error to be removed. A secondary, conventional adaptive optics system can be added after the hologram to remove any small amounts of aberration that may arise (see

Figure 11.1). It is worth stressing once again, that even with a perfect membrane mirror, there would still be the need for such a corrective system due to these same temporal effects.

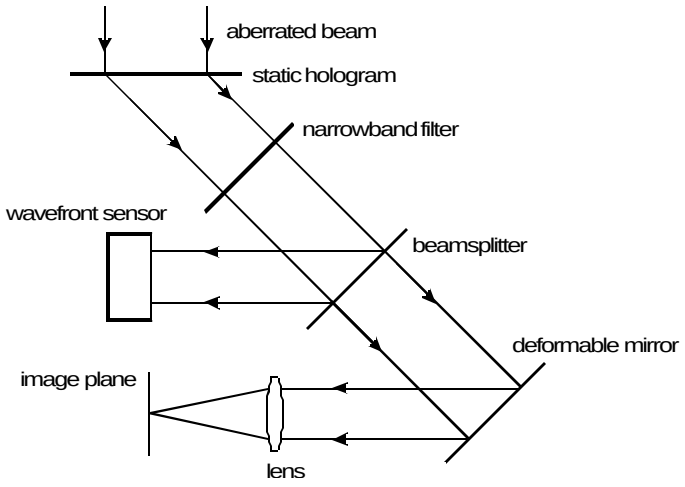

Fig. 11.1. Real-time holographic correction. This figure shows the addition of a simple adaptive optics system applied to a holographically corrected telescope. The large-scale aberrations are removed by a static hologram, while temporal changes in the mirror are corrected by the small-stroke, deformable mirror.

Under this task, we will use an adaptive optics module at the USAF Academy Laser and Optics Research Center (LORC) in Colorado Springs in conjunction with a holographic correction system (already setup) to test the 1m diameter membrane mirror built for the NRO. The membrane mirror is also already at the LORC. From this study, we will identify the parameters of the adaptive optics system and its projected capabilities in the future to put a bound on what is achievable in terms of correcting any remaining mirror aberrations. The identification of the capabilities of the AO system will also dictate the requirements on the stiffness of the overall structure which in turn sets the requirement on the stiffness of the other sub-components

Task 3. Thermal Analysis. Once the specific mission is identified, in this case the TPF, the orbit is likewise identified. Hence, the thermal sources and thermal loads on the components of the 100m diameter HCMT can be easily determined and used in a thermal analysis. Codes TRASYS and SINDA will be used for this task. The result of the thermal analysis on a 100m HCMT will tell us what temperature and temperature gradient to expect on-orbit. The two thermal codes mentioned above are workhorses of the industry and give fairly accurate predictions. Of course this is on the assumption that the codes have been given the right material and optical properties. L'Garde has a library of material and optical properties for every material we have used in the past.

Task 4. Finite element simulation. The 100m HCMT structure is nonlinear. The membrane mirror by itself is made of nonlinear material and because it experiences

deflections that are large relative to its thickness, geometric nonlinear finite element analysis must be used. Under this task, we will determine the *error budgets* that need to be assigned to each manufacturing, material, and environmental parameters that affect the overall surface accuracy. Here is where L'Garde's FAIM (Finite Element Analyzer for Membranes) code is useful. FAIM was written specifically for membrane structures. It has material and geometric nonlinear capability. We have also shown that in so far as nonlinear static membrane analysis is concerned, FAIM is more robust than commercially available codes.

The desired final surface figure of the membrane mirror is a paraboloid surface under tension. In order to be able to fabricate an accurate surface, we must know what the unstressed membrane surface looks like; i.e. we must solve the inverse problem. What must be the initial shape of the membrane so that after it is loaded to its final configuration, we have an accurate parabolic mirror? We have already solved this problem and the equations have been coded into our FLATE code. Large membrane mirrors and reflectors are usually fabricated using flat gores. In order to increase the accuracy even more, we also propose to investigate and analyze how much we gain in accuracy if formed gores are used for the 100m diameter HCMT.

Task 5. Increasing the operating bandwidth. The bandwidth of the telescope will be set by the severity of the aberrations initially present in the primary mirror, as well as the operating wavelength. For example, let us assume the bandwidth after correction is ±5nm, centered on the recording wavelength of 500nm (green) for a tenth of a wave performance. For wavelengths outside this bandwidth, the residual aberration will be larger than a tenth of a wave due to over or under correction of the mirror distortions (corresponding to red or blue wavelengths respectively).

There are three ways of approaching this problem[*]:

1. Construct multiple holograms of the mirror at different wavelengths in order to produce images in different parts of the spectrum,

2. Construct secondary holograms at a different wavelengths to the first, to correct for the aberrations present in the diffracted beam from the first hologram,

3. Use adaptive optics to alter the replay wavelength.

The first method is the simplest to understand. After passing through the imaging lens, the light is directed through a number of dichroic beamsplitters to separate out different wavelengths, which can then be used to form a number of different holograms. The drawback with this concept is that it will require a multiple number of holograms, imaging/bounce optics, image-capture devices, and most importantly a distant laser beacon capable of delivering more than one wavelength of light.

[*] N.B. in each case the final bandwidth will still be the same as before, but the center wavelength will be altered so that a different part of the spectrum can be accessed.

The second method will also require a multi-line laser beacon. With the primary hologram recorded in the green, say, illumination with a red laser beacon will result in an aberrated red beam. This beam is then sent onto a second holographic plate where a new hologram is recorded in the same manner as the first. Reconstruction can now be made at either the green wavelength, using only the first hologram, or in the red, using both.

The third scheme is perhaps the simplest. We once again have a single hologram that can correct for a narrow bandwidth in the green, but fails to completely correct for mirror aberrations in the red. The partially aberrated red beam is sent onto a deformable mirror that is actively controlled to remove the remaining wavefront aberrations. This will work only if the severity of the distortions at this wavelength is not too large. Although it is difficult to find acceptable holographic media sensitive to long wavelengths, this hybrid method may be a simple way in which infrared operation may be achieved. A further benefit of this method is that although it is difficult to construct bright laser sources operating at important astronomical emission lines (e.g. Lyman-alpha, Sodium D1&D2), the adaptive optics system can be used to shift the bandwidth to coincide with them. The resulting narrow, *tunable imaging bandwidth* will also make it possible to do some broad-range spectroscopic analysis of astronomical phenomena.

We will propose to investigate the third scheme.

Task 6. Beacon spacecraft station keeping and pointing. The requirements on the companion laser beacon spacecraft station keeping and pointing will be determined under this task. The issues include (a) distance between the beacon and the HCMT, (b) the laser beacon power required, and (c) pointing accuracy. The laser beacon platform is expected to be an independently controlled platform, co-orbiting with the telescope. The laser would have a series of capacitor banks that could be charged by small amounts of current over the long periods of idle time between operation. The laser will most likely be a Q-switched system with a pulse length of around 10ns. The precise laser power depends entirely on the size and medium chosen for the hologram. The restriction on the beacon wavelength is that a hologram can actually be recorded. Thus the wavelength is determined mostly by the sensitivity of the medium chosen. It is expected that multi-line operation will be desired, so there will need to be some method for converting the natural laser emission wavelength into other wavelengths. This can be achieved by Raman shifting in a multi-stage laser.

Task 7. Generate technology roadmap. In order to create the technology roadmap, we must first identify the enabling technologies for the 100m HCMT. As we proceed with the task of designing the 100m HCMT, we will identify any other enabling technologies that come up. We will use the predicted maturation points of the identified enabling technologies as milestones along the roadmap timeline culminating in the development, fabrication, and flight of a 100m holographically corrected membrane telescope. The enabling technologies we have identified so far include (during the performance of Phase II, we may identify more):

(A) Zero-CTE thin film materials. PBO has a very low CTE (-1 ppm/C) and will work but a zero-CTE membrane material will be even better.

(B) Fabricating a 100m diameter deployable membrane mirror with surface accuracy on the order of $\varepsilon \sim 1$ mm rms will be a challenge. Developing the technology to achieve this accuracy for 100m apertures is key to a working space-based HCMT.

(C) Due to the material nonlinearity, the (geometric) nonlinear nature of the statics (large deformation) of the large aperture telescope, the need to know its dynamic behavior, coupled with the fact that is size is many orders of magnitude larger than the surface accuracy desired, existing analytical codes may have to be modified or new ones written.

(D) We also need to develop space environment resistant rigidizable materials for the support structure. The LRA program is currently addressing the issues associated with this type of materials. For example, LRA is looking into synthesizing a Sub-Tg resin (for composite materials) with Tg in the neighborhood of –15C. At room temperature, which is about 35 C above this Tg, a woven graphite fabric impregnated with this resin will be foldable and packageable. When used in its operating environment, the material is passively cooled to a temperature of a few tens of degrees below its Tg (> 50 C below its Tg). Under these conditions, the material is stiff and rigid. Measurements show that under these conditions, it is possible to get modulus values for the composite on the order of a few million psi. The LRA program has already synthesized a space environment resistant Sub-Tg resin. It was tested at the Aerospace Corporation in El Segundo, California, and found to be radiation resistant to a total absorbed dose equivalent to a greater than 5 year life in a GEO orbit. It must also be pointed out the the Sub-Tg resins being considered have tailorable Tg; i.e., their glass transition temperatures can be moved up or down the temperature scale.

12.0 SUMMARY AND CONCLUSIONS

The objective of the Phase I study was to assess the feasibility of using ultra lightweight holographically corrected membranes as the primary mirror for a large aperture astronomical telescope. The conclusion of the study is that (a) holographically corrected membrane telescopes (HCMT) are eminently feasible and (b) they are the only **affordable** method today and in the foreseeable future enabling diffraction-limited space-based large aperture telescopes. We believe that the concept is revolutionary in the manner defined by the NASA Institute for Advanced Concepts (NIAC). If this concept were to be demonstrated for large apertures in space, and there is no reason why it could not be, it could revolutionize observational astronomy.

In a related NRO (National Reconnaissance Organization) study, a non-inflated 1m diameter parabolic membrane mirror was designed, fabricated, and measured to be within the 1 mm rms surface accuracy limit prescribed. The surface inaccuracy was measured to be $\varepsilon = 0.367$ mm rms which is well within that which could be fully corrected holographically. The NRO study has also proven, at least on a small scale, that the non-inflated net-less membrane mirror design is workable and can attain the required surface accuracy. Scalability to larger diameters was carried out analytically by performing a finite element simulation on 10m and 20m apertures. The analysis included the result of thermal calculations using TRASYS and SINDA. The results of the thermal calculations show that the use of extremely low CTE (coefficient of thermal expansion) PBO membrane combined with a sun-shielded telescope design results in low temperature gradients over the membrane mirror surface and temperatures remaining practically constant in time as long as the relative orientation between the sun and the telescope remains the same.

The 1m NRO membrane mirror was holographically corrected to the diffraction limit. After correction, the focal spot was diffraction limited. Its use as a diffraction-limited imaging device, was demonstrated by illuminating a USAF resolution chart with diffuse laser light and a photograph taken.

The perimeter truss design for the membrane mirror support structure is in Section 4.0. Here, we leveraged off the Large Radar Antenna (LRA) program with NASA/JPL. LRA is a current L'Garde program and is addressing the support structure materials and design for large space structures (~50m). The packaging and deployment control of large apertures will be addressed in detail during Phase II. The perimeter truss (PT) like the membrane mirror is foldable and packageable into a small launch volume. The PT is made of inflatably deployed material that rigidizes by passively cooling the structure to a temperature below its glass transition, Tg. The Tg of the resin used for the PT boom elements has been shown by the LRA program to be *tailorable*, up or down the temperature scale.

A conceptual design of a 1m diameter holographically corrected membrane telescope is presented in Section 9.0. The system issues are addressed and include (a) bandwidth, (b) temporal correction (fixed or real time holography), (c) holographic media, (d) laser beacon distance from the telescope, (e) laser beacon power and pointing requirements, and (f) laser beacon platform (co-orbiting or fixed). A conceptual design of the optics module is also presented. The overall conceptual design of a sun-shielded 1 m HCMT consists of the primary mirror, a holographic correction module, associated optics, and a co-orbiting laser beacon platform. Photopolymer material was chosen as the holographic medium because of its sensitivity to the laser frequency, high resolution, availability, low cost, heritage, and non-wet processing requirement. UV light is used to "fix" the hologram. For ultra high resolution research like planetary imaging, extraterrestrial planet search, deep sky surveys, etc., a more distant orbit such as the L2 Lagrange point would be required for lower thermal and gravitational gradients.

Finally, we outlined and listed some of the many applications of a narrow bandwidth telescope such as an HCMT. Very narrow band imaging and spectroscopy do have applications in astronomy but only for relatively bright sources. By using ultra lightweight membrane mirrors, we could increase the aperture diameter many fold to compensate for faint sources, without much mass penalty and launch vehicle constraint.

The applications address some of the NASA missions under the Space Science Enterprise (SPE) including (a) Search for Origins, (b) Structure and Evolution of the Universe, and (c) Exploration of the Solar System. Some of the applications considered are:

(K) Detection of extra-solar planets. The small angular separation between the planets and their host stars, as well as their extreme differences in brightness makes the detection very difficult. A large HCMT will make it possible to observe medium sized planets in the extra-solar neighborhood.

(L) Cosmology. Larger telescopes will allow us to resolve finer details and view fainter objects which in turn allows us to more accurately define the Hubble constant, the density of the universe, the cosmological constant (if it exists) and hence the age and future of the universe.

(M) Solar system objects. With a 100m diameter space telescope, we could observe every planet in our solar system with more detail than any previous fly by mission. We could also use the large telescope as an early warning device in finding and locating near-earth objects especially those that could intersect the earth's orbit around the sun.

(N) Black hole environs/accretion disks.

(O) Sun spots and solar flare activity on nearby stars.

(P) Red and brown dwarfs.

(Q) Galactic, stellar, and planetary formation regions.

(R) Astrometry. Astrometry requires high resolution measurement without the requirement of large bandwidth imaging. The number of stars observed by the Hipparcas/Tycho mission conducted by the European Space Agency (ESA) was ultimately limited by the size of the telescope aperture. For future catalogs, essential in the era of ultra large telescopes, large aperture astrometry missions will be required. HCMTs are well suited to this application.

(S) Optical communications. Experiments have shown that holographically corrected telescopes can be used for optical transmitters/receivers. In fact, as a consequence of the hologram, which is both a narrowband phase plate as well as a dispersive element, HCTs have the potential to isolate signal frequencies much better than conventional telescopes and with fewer optical elements. Signal bandwidths of 100 GHz have been demonstrated with >60dB blocking, with further improvements possible with holographic media.

(T) Lidar. Lidar involves the detection of scattered laser signal from some distant source. Since this source is often gaseous, the return signals are often so low that either a large laser pulse or large receiver (or both) is required. A large receiver can reduce the required laser power required. The results from optical communications tests show that HCTs can be used for lidar receivers, with many improvements over existing systems.

For astronomy, perhaps the most intriguing science would be due to the unexpected. Most discoveries made with new telescopes have been due to seeing the previously unobserved. We know the Hubble Deep Field showed images of galaxies far younger than other telescopes have detected before and with a dramatic increase in both resolution and light gathering power. An ultra large telescope aided by the membrane primary mirror and a holographic correction as outlined in this report will no doubt see a host of new objects and processes in our mysterious universe.

13.0 REFERENCES

1. Andersen, G., and Knize, R.J., "Holographically Corrected Telescopes", Proc. SPIE, Space Telescopes and Instruments V, Kona, Hawaii, March 25-28, 1998.

2. Andersen, G., Munch, J., and Veitch, P., "Compact holographic correction of aberrated telescopes", Appl. Opt. 36, 1427-1432 (1997).

3. Palisoc, A.L. and Cassapakis, C., "On Inflatable Antenna State-of-the-Art Precision", Proc. IEEE Ant. And Prop. Soc., International Symposium 1999, Orlando, Florida, July 11-16, 1999.

4. Denisyuk, Y.N. and soskin, S.I., "Holographic correction of deformational aberrations of the main mirror of a telescope", Opt. Spectrosc., 31, 535-538 (1971).

5. Soskin, S.I., and Denisyuk,Y.N., "Holographic correction of optical system aberrations caused by main-mirror deformation", Opt. Spectrosc., 33, 544-545 (1972).

6. Munch, J., Wuerker, R., and Heflinger, L., "Wideband holographic correction of an aberrated telescope objective", Appl. Opt. 29, 2440-2445 (1990).

7. Andersen, G., Munch, J., and Veitch, P., "Holographic correction of large telescope primaries using proximal, off-axis beacons", Appl. Opt., 35, 603-608 (1996).

8. Andersen, G. and Knize, J., "Holographically corrected telescope for high bandwidth optical communications", Appl. Opt., 38, 6833-6835 (1999).

9. Gruneisen, M.T., et al., "Holographic correction of severe dynamic aberrations in membrane-mirror based telescope systems", Proc. SPIE 3760, 142-152 (1999).

10. Wick, D.V., et al., "Deformed-helix ferroelectric liquid-crystal spatial light modulator that demonstrates high diffraction efficiency and 370-line pairs/mm resolution", Appl. Opt, 38, 3798-3803 (1999).

11. Smothers, W.K., et al., "Photopolymers for holography", Proc. SPIE, 1212, 20-39 (1990).

12. Rhee, U., et al., "Dynamics of hologram recording in DuPont photopolymer", Appl. Opt., 34, 846-853 (1995).

13. Volodin, B.L., et al., "Highly efficient photorefractive polymers for dynamic holography", Opt. Eng. 34, 2213-2223 (1995).

14. Stuckey, Meshishnek, Hanna, & Ross, "Space Environment Test of Materials for Inflatable Structures", The Aerospace Corp. Prepared for Space & Missile Systems Center.

16. Dr. Koorosh Guidanean, Materials Scientist, L'Garde, Inc., private communication, July 2000.

17. TRASYS - Thermal Radiation Analyzer System, COSMIC, University of Georgia, Athens, Georgia.

18. SINDA - Systems Improved Numerical Differencing Analyzer, COSMIC, University of Georgia, Athens, Georgia.

19. C. Patterson, I. Munro and J.C. Dainty, "A low cost adaptive optics system using a membrane mirror," Opt. Exp. **6**, 175-180 (2000).

20. P. Dayton et al., "Laboratory and field demonstration of low cost membrane mirror adaptive optics system," Opt. Comm. **176**, 339-345 (2000).

21. G. Andersen, J. Munch and P. Veitch, "Holographic correction of large telescope primaries using proximal, off-axis beacons," Appl. Opt. **35,** 603-608 (1996).

22. Anderson, G., "Holographic Correction of Large Aberrated Telescopes", Ph.D. Theses, University of Adelaide, Australia, 1996.

23. Smothers, W.K., et al., "Photopolymers for holography", Proc. SPIE 1212, 20-39 (1990).

24. Rhee, U., et al., "Dynamics of hologram recording in Du Pont Photopolymer", Appl. Opt. 34, 346-853 (1995).

25. Volodin, B.L., "Highly Efficient Photorefractive Polymers for Dynamic Holography", Opt. Eng., 34, 2213-2223 (1995).

26. Wick, D.V., et al., "Deforemed-helix ferroelectric liquid crystal spatial light modulator that demonstrates high diffraction efficiency and 370 line pairs/mm resolution", Appl. Opt., 38, 3798-3803 (1999).

27. Stockman, Jr., H.S., "Next Generation Space Telescope", The Association of Universities for Research in Astronomy, Inc., 1997.

14.0 ADDENDA SECTION FOR FUTURE HOLOGRAPHIC CORRECTION RESULTS